A GENERALIZED GRAPHICAL PRESENTATION OF MAGNETOHYDRODYNAMIC ACCELERATOR AND GENERATOR PERFORMANCE CHARACTERISTICS

W. L. Powers
ARO, Inc.
and
J. B. Dicks and W. T. Snyder
University of Tennessee Space Institute

October 1965

PROPULSION WIND TUNNEL FACILITY
ARNOLD ENGINEERING DEVELOPMENT CENTER
AIR FORCE SYSTEMS COMMAND
ARNOLD AIR FORCE STATION, TENNESSEE

NOTICES

When U. S. Government drawings specifications, or other data are used for any purpose other than a definitely related Government procurement operation, the Government thereby incurs no responsibility nor any obligation whatsoever, and the fact that the Government may have formulated, furnished, or in any way supplied the said drawings, specifications, or other data, is not to be regarded by implication or otherwise, or in any manner licensing the holder or any other person or corporation, or conveying any rights or permission to manufacture, use, or sell any patented invention that may in any way be related thereto.

Qualified users may obtain copies of this report from the Defense Documentation Center.

References to named commercial products in this report are not to be considered in any sense as an endorsement of the product by the United States Air Force or the Government.

A GENERALIZED GRAPHICAL PRESENTATION OF MAGNETOHYDRODYNAMIC ACCELERATOR AND GENERATOR PERFORMANCE CHARACTERISTICS

W. L. Powers
ARO, Inc.
and
J. B. Dicks and W. T. Snyder
University of Tennessee Space Institute

FOREWORD

The research effort reported herein was sponsored by the Arnold Engineering Development Center (AEDC), Air Force Systems Command (AFSC), under Program Element 62410034, Project 7778, Task 777805.

The research study presented was conducted by ARO, Inc. (a subsidiary of Sverdrup and Parcel, Inc.), contract operator of AEDC, AFSC, Arnold Air Force Station, Tennessee, under Contract AF 40(600)-1200, and the University of Tennessee Space Institute. The research was performed under ARO Project Number PL2287, and the manuscript was submitted for publication on August 18, 1965.

The authors wish to express their appreciation to W. R. Wimbrow and K. E. Tempelmeyer for suggesting an investigation of the diagonal conducting wall accelerator which led to the present work. Special thanks are due Dr. A. A. Mason and Dr. L. E. Ring for their numerous helpful suggestions and discussions. The authors further acknowledge A. K. Windmueller for many stimulating discussions and constructive criticisms and for providing the typical operating conditions of a large scale joint generator-accelerator experiment.

This technical report has been reviewed and is approved.

Robert H. LaBounty
1st Lt, USAF
Technology Division,
Experimental Branch
DCS/Plans and Technology

Donald D. Carlson
Colonel, USAF
DCS/Plans and Technology

ABSTRACT

This report presents a graphical display of the generalized Ohm's law which is assumed to describe the local electrical characteristics of magnetohydrodynamic accelerators and generators. Sheath voltage drops and ion slip are included, but viscous effects are excluded. A performance map is presented in terms of dimensionless electrical quantities. The features of the continuous electrode, segmented Faraday, segmented diagonal conducting wall, and segmented Hall accelerators and generators are represented on the same performance map for purposes of comparison. The operating equations pertinent to each of the special devices are also derived and expressed in terms of the dimensionless quantities. It is shown how this map may be used in evaluating MHD channel performance and how it materially aids in channel design and in selecting the most desirable kind of device for a given set of specifications.

CONTENTS

ILLUSTRATIONS

NOMENCLATURE

A	Channel cross-sectional area
$\vec{B}$	Magnetic induction
b	Ion slip factor, $2\left(\frac{N}{n+N}\right)^2 (\omega_i \tau_i)(\omega_e \tau_e)$
C	Constant for the constant total current, segmented diagonal conducting wall device, $I/A\,\sigma(uB + E_s)$
d	Channel transverse dimension
$\vec{E}$	Electric field intensity relative to the laboratory
$\vec{E}'$	Electric field intensity relative to the gas, $\vec{E} + \vec{u} \times \vec{B} - \hat{y} E_s$
E_s	Channel averaged sheath electric field, $\frac{V_s}{d} \frac{\vec{J}_y}{\lvert J_y \rvert}$
e	Electronic charge
e_i	Dimensionless component of electric field, $E_i/(uB + E_s)$ $(i = x \text{ or } y)$
I	Total current
$\vec{J}$	Current density
j_i	Dimensionless component of current density, $J_i/\sigma(uB - E_s)$ $(i = x \text{ or } y)$
K_A	Scaled accelerator efficiency, $(uB + E_s)\eta_A/uB$
K_G	Scaled generator efficiency, $1/K_A$

M	Ion Mass
m	Electron mass
N	Neutral particle number density
n	Electron number density
P	Dimensionless laboratory power density, $\vec{J} \cdot \vec{E}/\sigma\,(uB + E_s)^2$
$\vec{u}$	Gas velocity
V_s	Anode and cathode sheath voltage
$\hat{x}$	Unit vector in the x direction
$\hat{y}$	Unit vector in the y direction
$\hat{z}$	Unit vector in the z direction
α_g	Angle of the gas equipotential surface in the diagonal conducting wall device
α_w	Diagonal conducting wall angle, $\cot^{-1}\phi$
η_A	Local accelerator efficiency, $\vec{u} \cdot \vec{J} \times \vec{B}/\vec{J} \cdot \vec{E}$
η_G	Local generator efficiency, $1/\eta_A$
σ_o	Scalar conductivity, $n e^2 \tau_e/m$
σ	$\sigma_o/(1 + b)$
τ_e	Mean time between electron collisions
τ_i	Mean time between ion collisions
ϕ	Transverse to axial field ratio, E_y/E_x
Ω	$\frac{\omega_e \tau_e}{1 + b}$
ω_e	Electron cyclotron frequency, eB/m
ω_i	Ion cyclotron frequency, eB/m

SUBSCRIPTS

x	Axial component
y	Transverse component

SUPERSCRIPT

°	Limiting value

SECTION I
INTRODUCTION

The interaction of an electrically conducting gas with electric and magnetic fields is assumed to be given by the generalized Ohm's law. This equation is derived and discussed in detail in Section 6.4 of Cowling (Ref. 1) for a partially ionized and electrically neutral gas. Most workers simplify the equation by assuming that the plasma is homogeneous and neglecting electric pressure gradients and gravity. The generalized Ohm's law with these assumptions is written as

$$\vec{J} = \frac{\sigma_o}{1+b}\vec{E}' - \frac{\omega_e \tau_e}{(1+b)B}\vec{J} \times \vec{B} + \frac{b}{B^2(1+b)}(\vec{B} \cdot \vec{J})\vec{B} \qquad (1)$$

In the application of this equation to MHD accelerators and generators, the ion slip term, b, defined by Brunner (Ref. 2), in most cases is small. Harris and Cobine (Ref. 3) and Rosa (Ref. 4) point out that, in general, this ion energy dissipation term has little effect until $\omega_e \tau_e$ exceeds ten.

There is much work reported in the literature on the application of this equation to a specific type of accelerator or generator and for particular operating conditions. Celinski (Ref. 5) applies this equation to three kinds of MHD generators and uses vector diagrams to display the electrical characteristics. It has recently been brought to the attention of the authors that Burgel (Ref. 6) performed a somewhat similar treatment for the generator.

The purpose of this study is to devise a means of exhibiting the electric fields, currents, accelerating power density, laboratory power density supplied to or delivered by the gas, and the efficiency of all types of MHD accelerators and generators. In order to be of more use in practice, the equations are written in terms of the electric fields measurable in the laboratory, and the electrical sheath voltage drops adjacent to the electrodes are included. Limiting Hall electric fields, which cannot be exceeded because of breakdown considerations, are included for segmented devices. The treatment is special in the sense that no current is allowed in the direction of the magnetic field. This makes the last term in Eq. (1) zero. This display of Ohm's law can then be used to indicate performance trends of a particular device as well as comparisons between various kinds of devices which cannot readily be seen from the analytical expressions.

SECTION II
DERIVATION OF EQUATIONS

A right-hand Cartesian coordinate system is defined for both the accelerator and generator with the x-axis in the direction of the gas velocity $\vec{u}$, the y-axis in the direction transverse to the channel, and the z-axis in the direction of the magnetic induction as shown in Fig. 1. With $\hat{x}$, $\hat{y}$, and $\hat{z}$ as unit vectors along their respective axes, the relations are written as:

$$\begin{aligned}
\vec{B} &= \hat{z}\, B \\
\vec{u} &= \hat{x}\, u \\
\vec{J} &= \hat{x}\, J_x + \hat{y}\, J_y \\
\vec{E}' &= \hat{x}\, E_x' + \hat{y}\, E_y' \\
\vec{u} \times \vec{B} &= -\hat{y}\, u B \\
\vec{J} \times \vec{B} &= B(\hat{x}\, J_y - \hat{y}\, J_x) \\
\vec{E} \times \vec{B} &= B(\hat{x}\, E_y' - \hat{y}\, E_x')
\end{aligned} \tag{2}$$

The electric field $\vec{E}'$ as seen by the gas is written in terms of the electric field $\vec{E}$ measured in the laboratory.

$$\vec{E}' = \vec{E} + \vec{u} \times \vec{B} - \hat{y}\, E_s \tag{3}$$

where E_s is the channel averaged sheath electric field.

The components of the electric field become

$$E_x' = E_x, \quad E_y' = E_y - uB - E_s \tag{4}$$

The equations are simplified by defining the following relations:

$$\Omega \equiv \frac{\omega_e \tau_e}{1 + b}, \quad \sigma \equiv \frac{\sigma_o}{1 + b} \tag{5}$$

The electric field components are expressed in terms of the current components from Eqs. (1) through (5) as

$$\begin{aligned}
E_x &= \frac{1}{\sigma}\,(J_x + \Omega\, J_y) \\
E_y &= \frac{1}{\sigma}\,(J_y - \Omega\, J_x + \sigma\, uB + \sigma\, E_s)
\end{aligned} \tag{6}$$

The current components are expressed in terms of the electric field components as

$$J_x = \frac{\sigma}{1+\Omega^2}\left[E_x - \Omega\,(E_y - uB - E_s)\right]$$

$$J_y = \frac{\sigma}{1+\Omega^2}\left[E_y - uB - E_s + \Omega E_x\right] \tag{7}$$

The power density supplied to the Lorentz acceleration of the gas is given by $\vec{u} \cdot \vec{J} \times \vec{B}$. This is written in terms of either the current or electric fields as

$$\vec{u} \cdot \vec{J} \times \vec{B} = uB\,J_y = \frac{\sigma\,uB}{1+\Omega^2}\,(E_y - uB - E_s + \Omega E_x) \tag{8}$$

The power density input in the laboratory system is $\vec{J} \cdot \vec{E}$ and can be written in terms of the currents using Eq. (6) or in terms of the fields using Eq. (7) as

$$\vec{J} \cdot \vec{E} = \frac{1}{\sigma}\left[J_x^2 - J_y^2 + \sigma\,J_y\,(uB + E_s)\right]$$

$$= \frac{\sigma}{1+\Omega^2}\left[E_x^2 + E_y^2 + (\Omega E_x - E_y)(uB + E_s)\right] \tag{9}$$

In an accelerator, the input laboratory power density and the power density supplied to the gas motion are positive since J_y is positive. The local accelerator efficiency η_A is defined as the ratio of the power density supplied in the actual acceleration of the gas to the laboratory input power density. This is written in terms of the currents or fields as

$$\eta_A \equiv \frac{\vec{u} \cdot \vec{J} \times \vec{B}}{\vec{J} \cdot \vec{E}} = \frac{\sigma\,uB\,J_y}{J_x^2 + J_y^2 + \sigma\,J_y\,(uB + E_s)}$$

$$= \frac{uB(E_y - uB - E_s + \Omega E_x)}{E_x^2 + E_y^2 + (\Omega E_x - E_y)(uB + E_s)} \tag{10}$$

In a generator, $\vec{u} \cdot \vec{J} \times \vec{B}$ and $\vec{J} \cdot \vec{E}$ are negative since J_y is negative; the gas is decelerated, and power is delivered to the laboratory. The local generator efficiency η_G is defined as the ratio of the power density delivered to the laboratory to the power density taken from the gas motion.

$$\eta_G \equiv \frac{\vec{J} \cdot \vec{E}}{\vec{u} \cdot \vec{J} \times \vec{B}} = \frac{1}{\eta_A} \tag{11}$$

It is desirable to plot the accelerator and generator power densities and efficiencies as a function of J_x and J_y for a given σ, u, B, and E_s, and

also as a function of E_x and E_y for a given u, B, E_s, and Ω. It is noted that the power densities and efficiencies are independent of Ω when written in terms of the currents. This becomes the preferred representation; otherwise, there would be an infinite number of electric field representations for the system of all values of Ω.

SECTION III
DIMENSIONLESS QUANTITIES

The equations are simplified by defining the following dimensionless currents and electric fields:

$$j_x \equiv \frac{J_x}{\sigma(uB + E_s)}, \quad j_y \equiv \frac{J_y}{\sigma(uB + E_s)}$$

$$e_x \equiv \frac{E_x}{uB + E_s}, \quad e_y \equiv \frac{E_y}{uB + E_s} \tag{12}$$

With these substitutions, Eq. (6) provides the transformation equations between e_x, e_y, and j_x, j_y.

$$e_x = j_x + \Omega\, j_y, \quad e_y = j_y + 1 - \Omega\, j_x \tag{13}$$

This may be written in spinor notation as

$$\begin{pmatrix} e_x \\ e_y \end{pmatrix} = \begin{pmatrix} 1 & \Omega \\ -\Omega & 1 \end{pmatrix} \begin{pmatrix} j_x \\ j_y \end{pmatrix} + \begin{pmatrix} 0 \\ 1 \end{pmatrix} \tag{14}$$

which demonstrates that the equations translate, rotate through the angle $\tan^{-1}\Omega$, foreshorten, and preserve angle. Equation (7) provides the inverse transformation

$$j_x = \frac{e_x - \Omega(e_y - 1)}{1 + \Omega^2}, \quad j_y = \frac{e_y - 1 + \Omega e_x}{1 + \Omega^2} \tag{15}$$

The e_x, e_y axes are now located in the preferred j_x, j_y plane. Equation (15) reveals that the origin of the e_x, e_y axes ($e_x = e_y = 0$) for any value of Ω is located in the j_x, j_y plane at

$$j_x = \frac{\Omega}{1 + \Omega^2}, \quad j_y = -\frac{1}{1 + \Omega^2} \tag{16}$$

The equation of the locus of this origin for all values of Ω is found by eliminating Ω between the transformation equations of Eq. (13) and completing the square giving

$$j_x^2 + \left(j_y + \frac{1}{2}\right)^2 = \left(\frac{1}{2}\right)^2 \tag{17}$$

Since Ω and hence j_x are always positive, this locus is a semi-circle of radius one-half located at $j_x = 0$ and $j_y = -1/2$ and lies in the positive j_x and negative j_y quadrant as exhibited in Fig. 2. The coordinates of all points of interest are given, and the locations of the origin of the e_x, e_y axes for various values of Ω are shown. Equation (13) gives the intersection of the e_x axis and the j_y axis at $e_x = -\Omega$ and $j_y = -1$. It also gives the intersection of the e_x axis and the j_x axis at $e_x = 1/\Omega$ and $j_x = 1/\Omega$. It further shows that the e_y axis intersects the origin of the j_x, j_y axes at $e_y = 1$; this point is used to determine the scale of the e_x, e_y axes. It is noticed that $e_x = -\Omega/2$ and $e_y = 1/2$ at the point $j_x = 0$ and $j_y = -1/2$.

SECTION IV
DIMENSIONLESS POWER DENSITY

The dimensionless substitutions allow a dimensionless laboratory power density to be defined from Eq. (9) which can be used for both the accelerator and generator.

$$P \equiv \frac{\vec{j} \cdot \vec{E}}{\sigma (uB + E_s)^2} = j_y^2 + j_y + j_x^2$$

$$= \frac{e_y^2 - e_y + e_x^2 + \Omega e_x}{1 + \Omega^2} \tag{18}$$

Completing the square in the current expression of Eq. (18) gives

$$j_x^2 + \left(j_y + \frac{1}{2}\right)^2 = \frac{4P + 1}{4} \tag{19}$$

which demonstrates for both the accelerator and generator that a given dimensionless power density can be drawn as a circle of radius $\sqrt{4P + 1/2}$ centered at $j_x = 0$ and $j_y = -1/2$. Completing the square in the field expression of Eq. (18) gives

$$\left(e_x + \frac{\Omega}{2}\right)^2 + \left(e_y - \frac{1}{2}\right)^2 = \frac{(1 + \Omega^2)(4P + 1)}{4} \tag{20}$$

which expresses P in terms of the fields as a circle of radius $\sqrt{(1 + \Omega^2)(4P + 1)}/2$ centered at $e_x = -\Omega/2$ and $e_y = 1/2$.

The above equations are used to demonstrate the following:

1. When P vanishes, Eq. (19) reduces to the circle given by Eq. (17); thus, the generator is bounded in the j_x, j_y plane by the circle of radius one-half centered at $j_x = 0$ and $j_y = -1/2$.
2. The accelerator occupies the entire positive j_y domain.

3. The remainder of the domain not occupied by the generator and accelerator is a braking region in which power is supplied and the gas is decelerated as sketched in Fig. 3. This region will receive no further discussion other than how to avoid it during accelerator operation.

4. The locus of the origin of the e_x, e_y axes coincides with the generator bounding circle as shown in Fig. 4 (the e_x, e_y axes are displayed for a Ω of 3).

5. Along the j_y axis, Eq. (18) shows that P vanishes when j_y is 0 and - 1; the former corresponds to open-circuit operation of either an accelerator or generator, and the latter corresponds to short-circuit generator operation.

6. The absolute value of the generator dimensionless axial current density never exceeds one-half. The absolute value of the generator short-circuit dimensionless transverse current density never exceeds unity.

7. The partial derivative of P with respect to j_x exhibits a minimum of P for any given j_y when j_x vanishes. For a given gas acceleration less power need be supplied, or for a given gas deceleration more power is delivered, when there is no axial current.

8. The partial derivative of P with respect to j_y exhibits a minimum of P for any given j_x when $j_y = -1/2$. The maximum generator power density of - 1/4 occurs with $j_x = 0$ and $j_y = -1/2$.

SECTION V
SCALED EFFICIENCIES

The dimensionless substitutions allow a scaled accelerator efficiency to be defined* from Eq. (10) as

$$K_A \equiv \frac{uB + E_s}{uB}\,\eta_A = \frac{j_y}{j_y^2 + j_y + j_x^2} = \frac{j_y}{P} = \frac{e_y - 1 + \Omega e_x}{e_y^2 - e_y + e_x^2 + \Omega e_x} \qquad (21)$$

*Another efficiency of interest is the accelerator conversion efficiency defined by

$$\eta_A^* \equiv \frac{\vec{u} \cdot \vec{j} \times \vec{B}}{\vec{j} \cdot (\vec{E} - \vec{E}_s)} = \eta_A \frac{uB}{uB - E_s \eta_A} = K_A \frac{uB}{uB + E_s (1 - K_A)}$$

Note that η_A^* is a monotonic function of K_A.

Completing the square in the current expression of Eq. (21) yields

$$j_x^2 + \left(j_y - \frac{1 - K_A}{2 K_A}\right)^2 = \left(\frac{1 - K_A}{2 K_A}\right)^2 \tag{22}$$

which demonstrates that a given scaled accelerator efficiency can be drawn as a circle of radius $(1 - K_A)/2 K_A$ centered at $j_x = 0$ and $j_y = (1 - K_A)/2 K_A$. The circles expressing K_A in terms of the fields are obtained in the same way, but this is unnecessary since the e_x, e_y axes have already been located in the preferred j_x, j_y plane.

A scaled generator efficiency is defined from Eq. (11) using the substitutions as

$$K_G \equiv \frac{1}{K_A} = \frac{uB}{uB + E_s}\eta_G = \frac{j_y^2 + j_y + j_x^2}{j_y} = \frac{P}{j_y} = \frac{e_y^2 - e_y + e_x^2 + \Omega e_x}{e_y - 1 + \Omega e_x} \tag{23}$$

Completing the square in the current expression of Eq. (23) yields

$$j_x^2 + \left(j_y + \frac{1 - K_G}{2}\right)^2 = \left(\frac{1 - K_G}{2}\right)^2 \tag{24}$$

which expresses the values of K_G as circles of radius $(1 - K_G)/2$ centered at $j_x = 0$ and $j_y = -(1 - K_G)/2$.

SECTION VI
PERFORMANCE MAP

The dimensionless power density circles as calculated from Eq. (19) are presented in the j_x, j_y plane of Fig. 5; increments of 0.5 for the accelerator and of 0.05 for the generator are used. The scaled accelerator efficiency circles as calculated from Eq. (22) are given in increments of 0.1 down to 0.4. The scaled generator efficiency circles are displayed in increments of 0.1 using Eq. (24). The dimensionless electric fields are drawn after an operating Ω is established.

This becomes the performance map which expresses the electrical parameters as defined for a unit volume of gas by the generalized Ohm's law. For a given value of Ω if any one of the four quantities (currents, fields, power density, or efficiency) is known, then the other three are easily obtained from the proposed map. It is noted from Eqs. (18), (21), and (23) that $K_A = j_y/P$ and $K_G = P/j_y$; therefore, the dimensionless transverse current becomes the dimensionless Lorentz power density that goes into acceleration or deceleration of the gas. From any point on the map this dimensionless power density is obtained by projecting onto the j_y axis.

The performance map of Fig. 5 encompasses all generators and accelerators; if the external batteries or resistors are specified, any accelerator or generator may be exhibited. If the physical situation is such that an additional relationship exists among the quantities K_A, K_G, P, e_x, e_y, j_x, or j_y, then each quantity is uniquely determined in terms of any one of the others.

This completes the development of the performance map. It is of interest to apply this to various devices and to investigate its usefulness in channel design and device selection. Four particular MHD devices (continuous electrode, segmented Faraday, segmented diagonal conducting wall, and segmented Hall) are discussed and presented on the same map for purposes of comparison. The dimensionless substitutions are also used to derive the operating equations pertinent to each of the special devices.

SECTION VII
THE CONTINUOUS ELECTRODE DEVICE

The continuous electrode generator discussed by Rosa and Kantrowitz (Ref. 7) operates with no axial electric field. This generator is shown in Fig. 6a; the corresponding accelerator is obtained by replacing the load resistance with an external emf. Dimensionless electric fields are placed on the performance map for a Ω of 3 to illustrate the particular devices. This device operates along the e_y axis of Fig. 7.

Since $e_x = 0$, K_A is written in terms of P, e_y, j_x, or j_y using Eqs. (20) and (21) as

$$K_A = \frac{2}{1 + \sqrt{1 + 4P(1 + \Omega^2)}} = \frac{1}{e_y} = \frac{1}{1 - j_x \left(\frac{1 + \Omega^2}{\Omega}\right)} = \frac{1}{1 + j_y (1 + \Omega^2)} \qquad (25)$$

The negative sign of the square root has been omitted since negative K_A's do not exist.

The relations for the generator are

$$K_G = \frac{1 \pm \sqrt{1 + 4P(1 + \Omega^2)}}{2} = e_y = 1 - j_x \left(\frac{1 + \Omega^2}{\Omega}\right) = 1 + j_y (1 + \Omega^2) \qquad (26)$$

remembering that j_y and P are negative. It should be noted that when the transverse electric field is fixed, the efficiency is fixed. The accelerator is not very practical at large values of Ω because of the rapid decrease in efficiency. It is also observed that a desired generator power density may be extracted at two efficiencies; the larger

corresponds to large load and small current, and the smaller corresponds to small load and large current.

It is of interest to find the maximum generator dimensionless power density and the corresponding values of the electrical parameters. These are obtained by setting the partial derivative of Eq. (18) with respect to e_y equal to zero and utilizing Eqs. (15) and (23), giving

$$P_{max} = -\frac{1}{4(1+\Omega^2)}, \quad K_G = e_y = \frac{1}{2}$$

$$j_x = \frac{\Omega}{2(1+\Omega^2)}, \quad j_y = -\frac{1}{2(1+\Omega^2)} \tag{27}$$

The use of dimensionless and scaled quantities has made the calculations for operating conditions of interest much easier. All of the equations may be rewritten in terms of the original quantities by using Eqs. (12), (18), and (21). One of the more important features of this visual display is that values may be read directly from the performance map of Fig. 7, and thus the need for the analytical expressions is reduced.

SECTION VIII
THE SEGMENTED FARADAY DEVICE

Steg and Sutton (Ref. 8) discuss the Faraday device shown in Fig. 6b. It operates with no axial current and is represented by the j_y axis of Fig. 7.

Since $j_x = 0$, the scaled efficiencies are simply expressed in terms of each of the other parameters as

$$K_A = \frac{1}{K_G} = \frac{1}{1+j_y} = \frac{1}{e_y} = \frac{1}{1+\frac{e_x}{\Omega}}$$

$$K_A = \frac{2}{1+\sqrt{1-4P}}, \quad K_G = \frac{1 \pm \sqrt{1+4P}}{2} \tag{28}$$

It is noticed that the efficiency is fixed when the transverse electric field is fixed. It is also observed that a given power density may be generated at two efficiencies. These are the maximum and minimum efficiencies attainable by any generator at this power density. The map demonstrates that for generators in general the scaled efficiency obeys the relation

$$\frac{1-\sqrt{1+4P}}{2} \leq K_G \leq \frac{1+\sqrt{1+4P}}{2} \tag{29}$$

In contrast, the accelerator efficiency decreases with increasing power density input. The partial derivatives of Eqs. (21) and (23) with respect to j_x show that K_A and K_G are maximum for any given j_y when j_x vanishes. Since P is a minimum under the same conditions, no device is more efficient than the Faraday. The maximum generator dimensionless power density and the corresponding values are

$$P_{max} = -\frac{1}{4}, \quad K_G = e_y = \frac{1}{2}$$

$$j_y = -\frac{1}{2}, \quad e_x = -\frac{\Omega}{2} \tag{30}$$

In practice there will often be an axial electric field for segmented electrode devices which cannot be exceeded because of breakdown considerations. This maximum field, e_x°, is demonstrated in Fig. 7 with an arbitrary value of e_x° of 2 for the accelerator and -2 for the generator. The limiting operating values expressed in terms of e_x° using Eq. (28) are

$$K_{A_{lim}}^\circ = \frac{1}{K_G^\circ} = \frac{1}{1 + \frac{e_x^\circ}{\Omega}}, \quad P^\circ = \frac{e_x^\circ (e_x^\circ + \Omega)}{\Omega^2}$$

$$j_y^\circ = \frac{e_x^\circ}{\Omega}, \quad e_y^\circ = 1 + \frac{e_x^\circ}{\Omega} \tag{31}$$

which are shown by the intersection of the e_x° line and the j_y axis.

SECTION IX
THE SEGMENTED DIAGONAL CONDUCTING WALL DEVICE

Dicks (Ref. 9) and Montardy (Ref. 10) discuss the segmented diagonal conducting wall device shown in Fig. 6c, which operates with a specified transverse to axial electric field ratio, $\phi = E_y/E_x = \text{constant}$. The angle of the diagonal wall with the channel axis is given by α_w, and the angle of an equipotential surface in the midstream of the gas is designated by α_g; the defining relations become

$$\tan \alpha_w = \frac{1}{\phi} = \frac{E_x}{E_y} \quad \text{and} \quad \tan \alpha_g = \frac{E_y}{E_y - E_s} \tan \alpha_w = \frac{E_x}{E_y - E_s} \tag{32}$$

The generator boundary can be described from Eq. (16) as $j_x + \Omega j_y = 0$, and from $j_x e_x + j_y e_y = 0$ with $e_y/e_x = \phi$ as $j_x + \phi j_y = 0$. Therefore the positive values of ϕ shown on the generator boundary of Fig. 7 coincide with the values of Ω. A $\phi = 1$ accelerator and a $\phi = -1$ generator are

sketched in Fig. 7 by drawing straight lines through the appropriate values of Ω and ϕ.

The fixed relation between e_x and e_y used with Eq. (13) provides the following relation between j_x and j_y:

$$e_y = \phi e_x , \quad j_x = \frac{(1 - \Omega\phi) j_y + 1}{\Omega + \phi} \tag{33}$$

Thus only one field and one current component need be specified at a given operating point. It is assumed that in practice e_x will be the preferred measurement; hence, the scaled efficiencies and dimensionless power density are written as

$$K_A = \frac{1}{K_G} = \frac{e_x(\Omega + \phi) - 1}{e_x[e_x(1 + \phi^2) + \Omega - \phi]} , \quad P = \frac{e_x[e_x(1 + \phi^2) + \Omega - \phi]}{1 + \Omega^2} \tag{34}$$

An equation between P and K_A is obtained from Eq. (34) giving

$$P = \frac{(\Omega + \phi)^2 - (2 + \Omega^2 + \phi^2) K_A \pm (\Omega + \phi) \sqrt{[K_A(\Omega - \phi) - (\Omega + \phi)]^2 - 4K_A(1 + \phi^2)}}{2(1 + \Omega^2)(1 + \phi^2) K_A^2} \tag{35}$$

which demonstrates that the diagonal wall accelerator can operate at the same efficiency for two different power densities. Setting the derivative of K_A with respect to e_x equal to zero gives the maximum K_A and the corresponding values to be

$$K_{A_{max}} = \left(\frac{\Omega + \phi}{\sqrt{1 + \Omega^2} + \sqrt{1 + \phi^2}} \right)^2 , \quad P = \frac{\left(\sqrt{1 + \Omega^2} + \sqrt{1 + \phi^2}\right)^2}{(\Omega + \phi)^2 \sqrt{(1 + \Omega^2)(1 + \phi^2)}}$$

$$e_x = \frac{\sqrt{1 + \Omega^2} + \sqrt{1 + \phi^2}}{(\Omega + \phi)\sqrt{1 + \phi^2}} , \quad j_y = \frac{1}{\sqrt{(1 + \Omega^2)(1 + \phi^2)}} \tag{36}$$

It is noticed that maximum efficiency for a given Ω and ϕ occurs with a finite axial current (Eq. (33)). This is consistent with the previous conclusion since the Faraday device at the same j_y is more efficient. Increasing the power density until j_x vanishes reduces the efficiency. The electrical characteristics of this device operating with $j_x = 0$ are

$$K_A = \frac{1}{K_G} = \frac{\Omega\phi - 1}{\Omega\phi} , \quad P = \frac{\Omega\phi}{(\Omega\phi - 1)^2}$$

$$e_x = \frac{\Omega}{\Omega\phi - 1} , \qquad j_y = \frac{1}{\Omega\phi - 1} \tag{37}$$

Equations for P and K_G are obtained from Eq. (34). The solution for P becomes

$$P = \frac{K_G[K_G(\Omega + \phi)^2 - (2 + \Omega^2 + \phi^2) \pm (\Omega + \phi)\sqrt{[K_G(\Omega + \phi) - (\Omega - \phi)]^2 - 4K_G(1 + \phi^2)}]}{2(1 + \Omega^2)(1 + \phi^2)} \tag{38}$$

which gives the two different power densities which can be generated at a given efficiency. The solution for K_G is

$$K_G = \frac{P[\,2+\Omega^2+\phi^2 \pm (\Omega+\phi)\sqrt{(\Omega+\phi)^2+4P(1+\Omega^2)(1+\phi^2)}\,]}{2[\,P(\Omega+\phi)^2-1\,]} \tag{39}$$

which shows that a given power density may be generated at two different efficiencies. Setting the derivative of K_G with respect to e_x equal to zero yields the maximum K_G and the corresponding values as

$$K_{G_{max}} = \left(\frac{\sqrt{1+\Omega^2}-\sqrt{1+\phi^2}}{\Omega+\phi}\right)^2, \quad P = -\frac{\left(\sqrt{1+\Omega^2}-\sqrt{1+\phi^2}\right)^2}{(\Omega+\phi)^2\sqrt{(1+\Omega^2)(1+\phi^2)}}$$

$$e_x = \frac{\sqrt{1+\phi^2}-\sqrt{1+\Omega^2}}{(\Omega+\phi)\sqrt{1+\phi^2}}, \quad j_y = -\frac{1}{\sqrt{(1+\Omega^2)(1+\phi^2)}} \tag{40}$$

The derivative of P with respect to e_x is set equal to zero giving the maximum generator dimensionless power density and the corresponding values as

$$P_{max} = -\frac{(\Omega-\phi)^2}{4(1+\Omega^2)(1+\phi^2)}, \quad K_G = \frac{(\Omega-\phi)^2}{2(2+\Omega^2+\phi^2)}$$

$$e_x = \frac{\phi-\Omega}{2(1+\phi^2)}, \quad j_y = -\frac{2+\Omega^2+\phi^2}{2(1+\Omega^2)(1+\phi^2)} \tag{41}$$

It should be noted that maximum efficiency operation and maximum power density operation of this generator are considerably different. It is also observed that maximum generator efficiency takes place with a finite axial current (Eq. (33)) as did the accelerator. The generator operating parameters with no axial current are given also by Eq. (37), remembering that ϕ is negative. In practice, all of the above operating values are more easily extracted from the performance map of Fig. 7.

The dimensionless current densities in the diagonal wall device at open-circuit conditions are given by Eq. (16) and are shown on the performance map at the point, $P = e_x = e_y = 0$. It is noted that the "accelerator" operates in the braking region between open-circuit conditions and zero efficiency conditions. The dimensionless parameters at $K_A = j_y = 0$ are

$$e_x = j_x = \frac{1}{\Omega+\phi}, \quad P = \frac{1}{(\Omega+\phi)^2} \tag{42}$$

To avoid this region, a dimensionless power density greater than that given above must be introduced. This criterion may be expressed in terms of the power density, $\vec{J} \cdot \vec{E}$, according to Eq. (18).

The effects of a limiting axial electric field are particularly interesting for this device. Both the accelerator and generator may

operate up to a breakdown field e_x° ; the limiting operating values are obtained by substituting the proper e_x° into Eqs. (15) and (34). These limiting values for $e_x^\circ = \pm 2$ are shown on the performance map of Fig. 8 for a Ω of 3. To generalize, the locus of the point $e_x = e_x^\circ$ and $e_y = \phi e_x^\circ$ is determined for the system of all values of Ω by eliminating Ω between the transformation equations (Eq. (13)) and completing the square giving

$$\left(j_x - \frac{e_x^\circ}{2}\right)^2 + \left(j_y - \frac{\phi e_x^\circ - 1}{2}\right)^2 = \left(\frac{e_x^\circ}{2}\right)^2 + \left(\frac{\phi e_x^\circ - 1}{2}\right)^2 \qquad (43)$$

These circles are sketched in Fig. 8 for both the accelerator and generator; they become operating envelopes separating the operation region from the breakdown region. The envelopes vary for each value of ϕ; the ones shown are for a $\phi = 1$ accelerator and a $\phi = -1/2$ generator. They show that diagonal wall accelerators operating at large values of Ω with the limiting axial field constraint are confined to low power densities; larger power densities may be introduced by decreasing the value of Ω with an accompanying efficiency decrease.

One interesting mode of operation of this diagonal wall device is with constant total current which permits a two-terminal connection to the external circuit. It is easily shown (Ref. 11) that the total current I may be written in terms of the current densities in the gas or in terms of the dimensionless currents as

$$I = A(J_x + \phi J_y), \quad C \equiv \frac{I}{A\sigma(uB + E_s)} = j_x + \phi j_y \qquad (44)$$

where A is the cross-sectional area, and C is a constant describing a straight line on the performance map. The operating parameters for a given set of ϕ, Ω, and C values are determined from Eqs. (13), (33), (34), and (44) to be

$$K_A = \frac{1}{K_G} = \frac{C(\Omega + \phi) - 1}{C[C(1 + \Omega^2) + \phi - \Omega]}, \quad J_y = \frac{C(\Omega + \phi) - 1}{1 + \phi^2}$$

$$P = \frac{C[C(1 + \Omega^2) + \phi - \Omega]}{1 + \phi^2}, \quad e_x = \frac{C(1 + \Omega^2) + \phi - \Omega}{1 + \phi^2} \qquad (45)$$

Consider, for example, an accelerator which is designed for a ϕ of 1 and a Ω of 4 as shown in Fig. 9. Suppose that when the operating values are introduced into Eq. (44), a value for C of 0.3 is obtained; this line is drawn on the map. The intersection of these two straight lines displays the resulting e_x, e_y, j_x, j_y, P, and K_A. Again, the need for the analytical expressions is reduced.

SECTION X
THE SEGMENTED HALL DEVICE

The segmented Hall device discussed by Karlovitz and Halász (Ref. 12) is shown in Fig. 6d. It operates with no transverse electric field and is represented by the e_x axis of Fig. 7.

The Hall device is a special case, $\phi = 0$, and has all the features of the diagonal wall device. The equations pertinent to this device are obtained by setting $\phi = 0$ in Eqs. (33) through (45). In practice, the performance map is more convenient than the equations.

The performance map shows that the Hall accelerator can operate at the same efficiency for two different power densities. The maximum K_A and the corresponding currents and fields are also shown in Fig. 7. There is no maximum power density input except that determined by a limiting axial electric field. The accelerator may pass over into the braking region; the operating conditions which should be avoided are indicated on the map.

Figure 7 shows that the Hall generator has two efficiencies for a given power density output; it also demonstrates the two power density outputs at a given efficiency. The maximum K_G and the corresponding electrical values are given. The maximum generator P and the corresponding parameters may also be picked off the map.

Operating envelopes for both the accelerator and generator similar to Fig. 8 may be drawn. The constant total current mode of operation similar to Fig. 9 becomes the straight line parallel to the j_y axis. The location of the operating point for a given value of Ω and C is obtained by the intersection of the $C = j_x$ line and the e_x axis. The currents in the segmented Hall device at open-circuit conditions ($P = j_x = e_y = 0$) are given by Eq. (16) and are shown on the performance map.

SECTION XI
USE IN GENERATOR SELECTION

In any MHD device, the electrical parameters vary down the channel and when the aerodynamic variables are included, a computer is required to calculate the overall performance. The map does materially aid, however, in channel design and in the selection of the most desirable type of device for a given set of specifications by visually providing the electrical

properties of a typical unit volume of gas in any device without resorting to the use of sometimes cumbersome equations.

A few generator types are investigated on the same performance map of Fig. 10. The continuous electrode, Faraday, and Hall generators are exhibited for $\Omega = 2$; two diagonal wall generators are shown: $\phi = -1/2\,(\alpha_w = -63\ \text{deg})$ and $\phi = -1\,(\alpha_w = -45\ \text{deg})$. There are several interesting points which are considered in the selection of a given device. Each generator has a particular point (a, b, c, d) corresponding to maximum dimensionless power density. Each generator has a point (f, g, h) corresponding to maximum efficiency. The limiting axial electric field prescribes points (ℓ, m, n, p) on all but the continuous electrode generator. The values of the dimensionless parameters at each point are tabulated for quick comparison.

Consider a gas with a given density, pressure, temperature, mass flow rate, and seed concentration under the following typical conditions:

$$\begin{aligned} B &= 2\ \text{weber/m}^2 & \sigma &= 20\ \text{mho/m} \\ u &= 2000\ \text{m/sec} & E_x^\circ &= -6000\ \text{v/m} \\ \Omega &= 2 & E_s &= 0 \end{aligned} \tag{46}$$

The scaled efficiency K_G then becomes the actual local efficiency η_G, and $e_x^\circ = E_x^\circ/uB = -1.5$. The laboratory fields, currents, and power density are obtained from the dimensionless quantities according to

$$\begin{aligned} \frac{E_x}{e_x} &= \frac{E_y}{e_y} = 4{,}000\ \text{v/m} \\ \frac{J_x}{j_x} &= \frac{J_y}{j_y} = 80{,}000\ \text{amp/m}^2 \\ \frac{\vec{J} \cdot \vec{E}}{P} &= 320\ \text{megawatt/m}^3 \end{aligned} \tag{47}$$

The first consideration will be the extraction of a large power density from the gas. The continuous electrode generator is not practical from a large power density standpoint for this value of Ω as shown at point c. The power density at point a is the largest that can be generated by any type of device; only the Faraday and the 63-deg diagonal wall generators may operate at this point. The fields and currents at point a are obtained from Eq. (47); $E_x = -4$ kv/m, $E_y = 2$ kv/m, $J_x = 0$, and $J_y = -40$ ka/m^2. The 63-deg diagonal wall generates a power density of 80 megawatt/m^3 at an efficiency of 50 percent. The Hall generator operating at point b has a power density of 64 megawatt/m^3 at an efficiency of

33 percent. The axial electric fields at points a and b are the same; therefore, with the same cross-sectional area, the Hall generator would have to be 25 percent longer than either the Faraday or 63-deg diagonal wall generator to produce the same total power output. This length increase will necessarily require a large magnet. Suppose 20 megawatts were required of the generator having a cross-sectional area of 0.1 m^2. The 63-deg diagonal wall could generate approximately 2000 amp at 10,000 v with a length of 2.5 m, whereas the Hall generator would produce 1600 amp at 12,500 v with a length of 3.12 m.

The second consideration will be operation at maximum efficiency. The Faraday and continuous electrode generators approach 100-percent efficiency with open-circuit conditions and have no maximum during power generation. The 63-deg diagonal wall generator operating at point g is 1.11 times more efficient but has only 89 percent of the power density as that operating at point a. Operation at point g is 1.45 times more efficient and has 1.3 times more power density than the Hall generator operating at point f. A Faraday generator could be operated at the same power density as the 63-deg diagonal wall at point g and would be 1.2 times more efficient. The 45-deg diagonal wall generator operating between points d and h has about the same efficiency as a Faraday with the same power density.

The third consideration will be the generation of a large voltage with a short channel. This requires as large an axial electric field as possible without breakdown. The Hall and the 63-deg diagonal wall generators operating at points ℓ and n both produce 12,000 v with a 2-m channel under the stated conditions. For a cross-sectional area of 0.1 m^2, the Hall generator produces approximately 9.6 megawatts at 800 amp, whereas the diagonal wall generator produces 12 megawatts at 1000 amp.

For purposes of comparison, the velocity, conductivity, and magnetic induction will be the same as before, but the value of Ω will be reduced to unity by approximately doubling the density. The Faraday, Hall, continuous electrode, and 45-deg diagonal conducting wall generators are exhibited in Fig. 11. As before, each generator has a particular point (a, b, c) corresponding to maximum dimensionless power density; the values at each point are tabulated for comparison. This particular diagonal wall generator was chosen to operate through the maximum power point. The effect of different values of Ω in the selection of a particular generator from a maximum power density standpoint is demonstrated by comparing points a, b, and c on Figs. 10 and 11. Decreasing the value of Ω from 2 to 1 decreases the axial electric field of the Faraday and diagonal wall generators at point a by 1/2 and increases the power density of the continuous electrode generator by 5/2 at point c. It

decreases the axial electric field and efficiency by 1/2 and decreases the power density by 5/8 at point b of the Hall generator.

It is interesting to note that with the same cross-sectional area, the 45-deg diagonal wall generator operating at point a with an Ω of 1 produces the same total power in the same length as the 63-deg diagonal wall with an Ω of 2, but with twice the current I and half the voltage.

The Hall generator operating at point b with an Ω of 1 would have to be 8/5 longer to produce the same total power as when operating with an Ω of 2; therefore, increasing the density of the Hall generator makes it less attractive. In contrast, this decrease in the value of Ω has made the continuous electrode generator more attractive; in fact, it now generates the same total power at point c in the same length as does the Hall at point b and with three times the efficiency. For a Ω of 1, and everything else the same, the Faraday and the 45-deg diagonal wall generators operating at point a need to have only half the length of either the Hall operating at point b or the continuous electrode operating at point c to produce the same total power.

SECTION XII
USE IN ACCELERATOR SELECTION

A few types of accelerators are shown in Fig. 12. The continuous electrode, Faraday, Hall, and $\phi = 1$ ($a_w = 45$ deg) diagonal wall accelerators are displayed along with a limiting e_x^o line for a value of Ω of 3. It is interesting to compare all the types at some specified input power density (a, b, c, d) as well as the maximum efficiency points (f, g). There are no maximum power density points for accelerators except those determined by the limiting axial electric field (ℓ, m, n).

At a given power density no accelerator is more efficient than the segmented Faraday. For P = 0.5, the Faraday at point a is 1.41 times more efficient than the Hall at point b and 2 times more efficient than the continuous electrode accelerator at point c. The 45-deg diagonal wall accelerator operating in the power density range between points d and n is about as efficient as the Faraday operating between points a and m.

Consider the following typical operating conditions:

$$\begin{aligned} B &= 1 \text{ weber/m}^2 & \sigma &= 100 \text{ mho/m} \\ u &= 2000 \text{ m/sec} & E_x^o &= 6000 \text{ v/m} \\ \Omega &= 3 & E_s &= 1000 \text{ v/m} \end{aligned} \tag{48}$$

In this case, the local efficiency η_A is 2/3 the scaled efficiency K_A, and the limiting dimensionless axial field e_x° is 2. The laboratory fields, currents, and power density are obtained from the dimensionless quantities according to

$$\frac{E_x}{e_x} = \frac{E_y}{e_y} = 3000 \text{ v/m}$$

$$\frac{J_x}{j_x} = \frac{J_y}{j_y} = 300{,}000 \text{ amp/m}^2$$

$$\frac{\vec{J} \cdot \vec{E}}{P} = 900 \text{ megawatt/m}^3 \qquad (49)$$

From Eq. (49) the total power which may be introduced into the various accelerators when operating at points ℓ, m, and n without axial breakdown can be calculated. Consideration should be given the operation of a channel 2 m long having a cross-sectional area of 0.02 m^2 under the given conditions by applying an axial voltage of 12,000 v. Approximately 36 megawatts could be introduced into the Hall accelerator with 33.3 percent of this going into gas acceleration; 40 megawatts could be put into the Faraday with 40 percent going into acceleration; and 43 megawatts could be introduced into the diagonal wall accelerator with an efficiency of 38.8 percent. With these channel dimensions, approximately 2.25 megawatts should be supplied to the diagonal wall accelerator, and approximately 4 megawatts should be put into the Hall accelerator to avoid braking the gas. Just a few applications of the performance map have been demonstrated; this by no means exhausts its possibilities.

SECTION XIII
THREE-DIMENSIONAL MODELS

Three-dimensional models of both the accelerator and generator performance characteristics may be constructed by adding the scaled efficiency as an altitude to the dimensionless current plane. The lines of intersections of constant efficiency planes with the efficiency surface are given by Eqs. (22) and (24). Equation (22) does not describe a developable surface since j_y varies from 0 to ∞ as K_A varies between 1 and 0; however, a partial surface may be constructed. Figure 13 is a photograph of the accelerator model presenting the scaled efficiency in intervals of 0.1 down to 0.4, which includes most MHD accelerators. The dimensionless currents are presented in intervals of 0.2 as background grid. The lines of intersection of the dimensionless laboratory

power density cylinders with the surface are given by Eq. (19) and are placed on the model in intervals of 0.5. The dimensionless electric fields are not drawn on the model until after an operating Ω is established. Equation (24) reduces to Eq. (17) when $K_G = 0$; $K_G = j_y + 1$, when $j_x = 0$; thus the generator efficiency surface is an oblique cone having its altitude as an element. The generator development is given in Fig. 14 for certain scaled efficiencies, dimensionless currents, and dimensionless power densities which may be cut out to obtain a working model. The performance map of Fig. 5 is the projection of these models onto the base plane.

These models are useful in providing a qualitative comparison of the various types of devices. Figure 15 is a photograph of the accelerator model showing the Hall, 45-deg diagonal wall, and Faraday accelerators for a Ω of 3, along with an e_x° limiting line of 2. Figure 16 is a photograph of the generator model exhibiting the Hall, 63-deg diagonal wall, and Faraday generators for a Ω of 2. The continuous electrode device is hidden from view in the photographs. Other three-dimensional models could be constructed by adding the dimensionless power density as the altitude to the dimensionless current plane and then locating the scaled efficiency and electric field lines.

SECTION XIV
CONCLUDING REMARKS

The entire presentation from a physical point of view is based on the assumption of the generalized Ohm's law, on the definitions of the accelerating power density, the laboratory power density, and the local efficiency. Rendering the currents and fields dimensionless greatly simplifies the resulting expressions and allows the construction of a performance map for both the accelerator and generator. The map is not limited to the four special types of devices which were considered; in fact, the map encompasses all devices. The operating equations pertinent to each of the special devices are also derived and expressed in terms of the dimensionless parameters.

The performance map is of more use in practice than the three-dimensional surfaces, since lines representing specific configurations can be drawn on it more easily, especially for various values of Ω. The map allows all devices to be shown together, and hence comparisons between various devices can be made. It materially aids in selecting the most desirable type of device for a given set of specifications. Values of the scaled and dimensionless quantities may be read directly

from the map, and hence the need for the analytical expressions is reduced. If any one of the four quantities (electric fields, currents, power density, or efficiency) is specified, then the other three are easily obtained from the map. For a given kind of device, the effect of varying values of Ω, ϕ, I, uB, E_s, etc., on the interesting operating points may be readily seen from the performance map.

REFERENCES

1. Cowling, T. G. Magnetohydrodynamics, Interscience Publishers, Inc., New York, 1957.
2. Brunner, M. J. "The Effects of Hall and Ion Slip on the Electrical Conductivity of Partially Ionized Gases for Magnetohydrodynamic Re-Entry Vehicle Application." Journal of Heat Transfer, Trans. ASME, Paper No. 61-WA-176. Presented at ASME Meeting Nov. 26 - Dec. 1, 1961.
3. Harris, L. P. and Cobine, J. D. "The Significance of the Hall Effect for Three MHD Generator Configurations." Journal of Engineering for Power, October 1961, p. 392.
4. Rosa, R. J. "Hall and Ion-Slip Effects in a Nonuniform Gas." Physics of Fluids, Vol. 5, September 1962, p. 1081.
5. Celinski, Z. "Analyse der Arbeit von Gleichstrom MHD Generatoren mit Stationaerer, linearer, Gasstroemung mit Hilfe von Vektordiagrammen." Institut fur Plasma Physik, Garching bei Muenchen, IPP 3/21, May 1964.
6. Burgel, B. "An Investigation of M.P.D. Generators by a Simplified Graphical Method." I.E.E. Conference Report, Series No. 4, Symposium on Magnetoplasmadynamic Electrical Power Generation, King's College, University of Durham, September 6-8, 1962.
7. Rosa, R. J. and Kantrowitz, A. "Magnetohydrodynamic Energy Conversion Techniques." Direct Conversion of Heat to Electricity, edited by J. Kaye and J. A. Welsh, John Wiley and Sons, Inc., New York, 1960.
8. Steg, L. and Sutton, G. W. "Prospects of MHD Power Generation." Astronautics, Vol. 5, August 1960, p. 22.
9. Dicks, J. B. "Improvements in Design of MHD Accelerator Channels for Aerodynamic Purposes." AGARD Specialists Meeting, Rhode-Saint-Genese, Belgium, September 21-23, 1964.

10. Montardy, A. de. "A MPD Generator with Series Connected Electrodes." I.E.E. Conference Report Series No. 4, Symposium on Magnetoplasmadynamic Electrical Power Generation, King's College, University of Durham, September 6-8, 1962.

11. Windmueller, A. K. ARO, Inc., AEDC, Private Communication.

12. Karlovitz, B. and Halász, D. "Process for the Conversion of Energy and Apparatus for Carrying Out the Process." U. S. Patent 2,210,918, August 13, 1940.

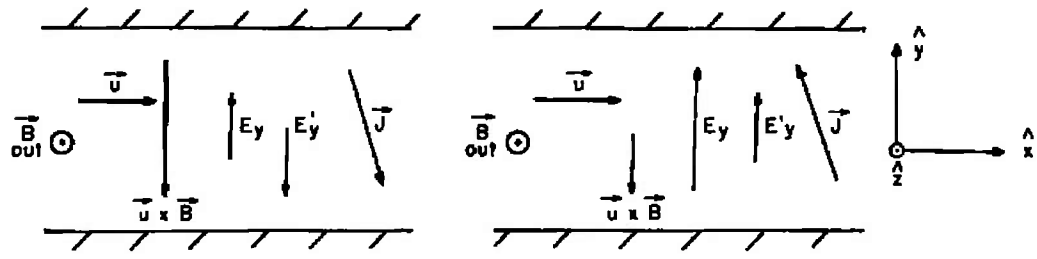

a. Generator Channel b. Accelerator Channel

Fig. 1 Coordinate System (Electrodes Not Shown)

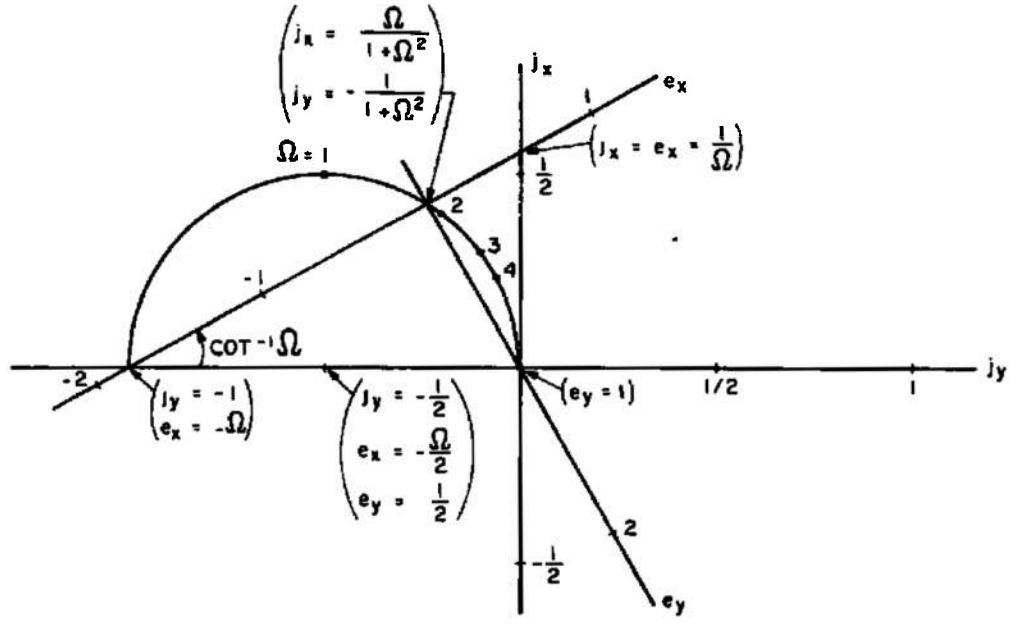

Fig. 2 Dimensionless Currents and Fields in the Same Plane

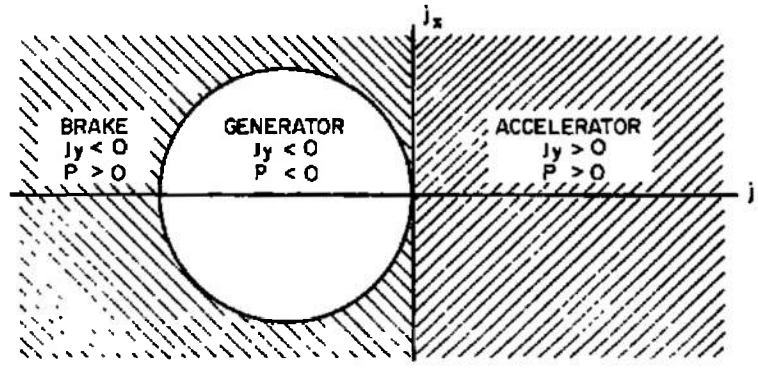

Fig. 3 Operating Domains

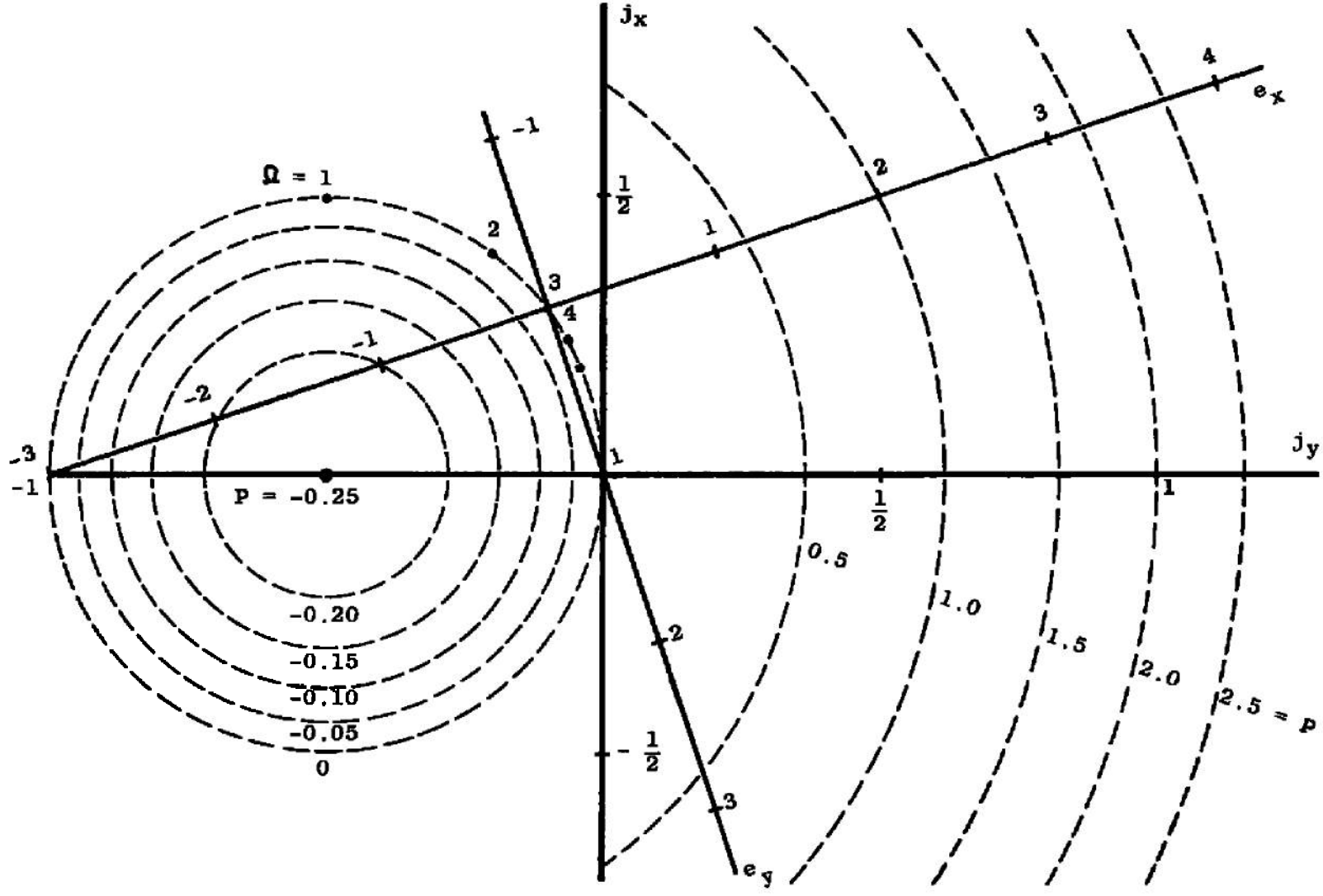

Fig. 4 Dimensionless Laboratory Power Density Circles

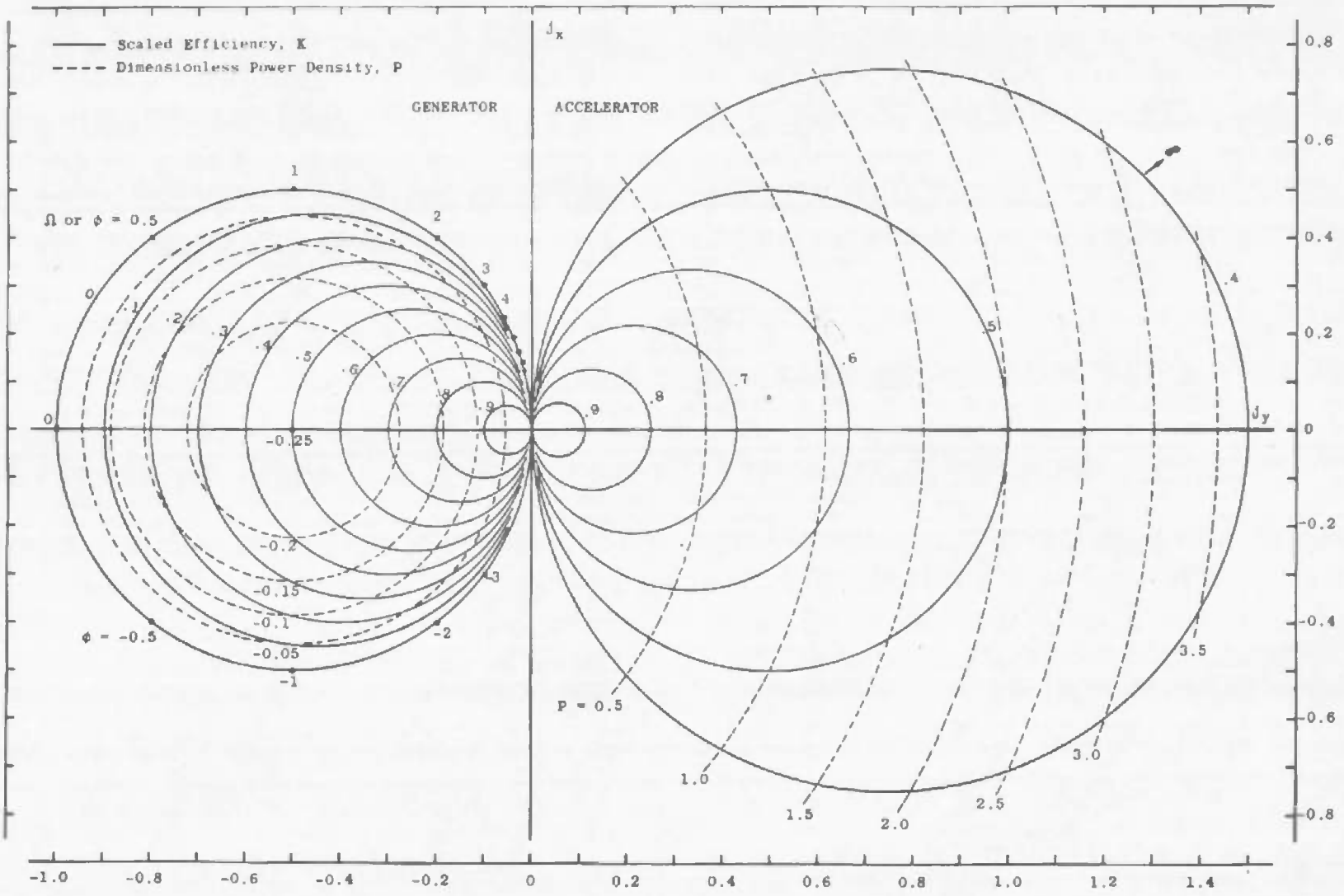

Fig. 5 Performance Map

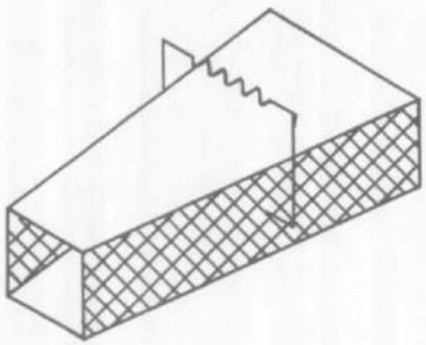

a. Continuous Electrode

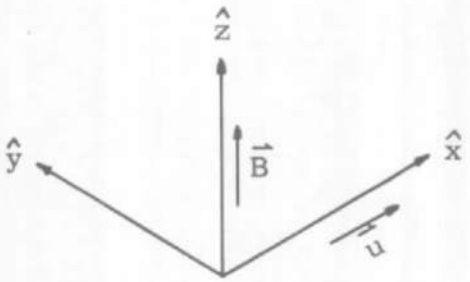

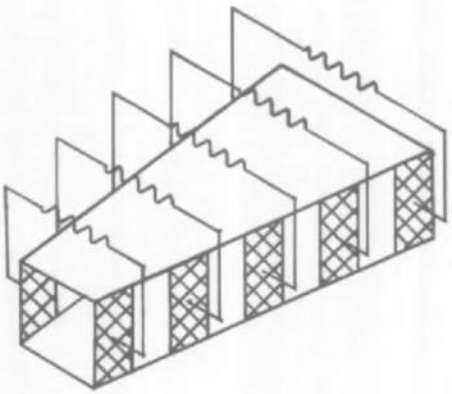

b. Segmented Faraday

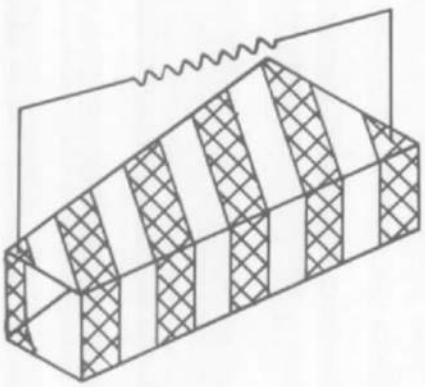

c. Segmented Diagonal Conducting Wall

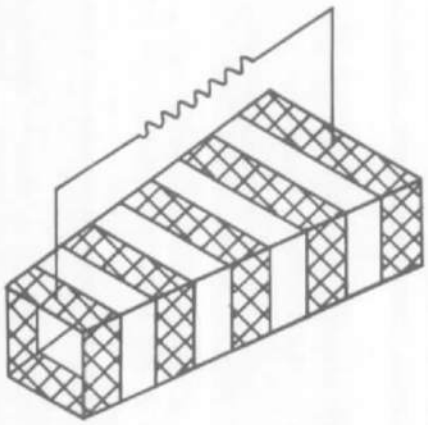

d. Segmented Hall

Fig. 6 MHD Generator Designs

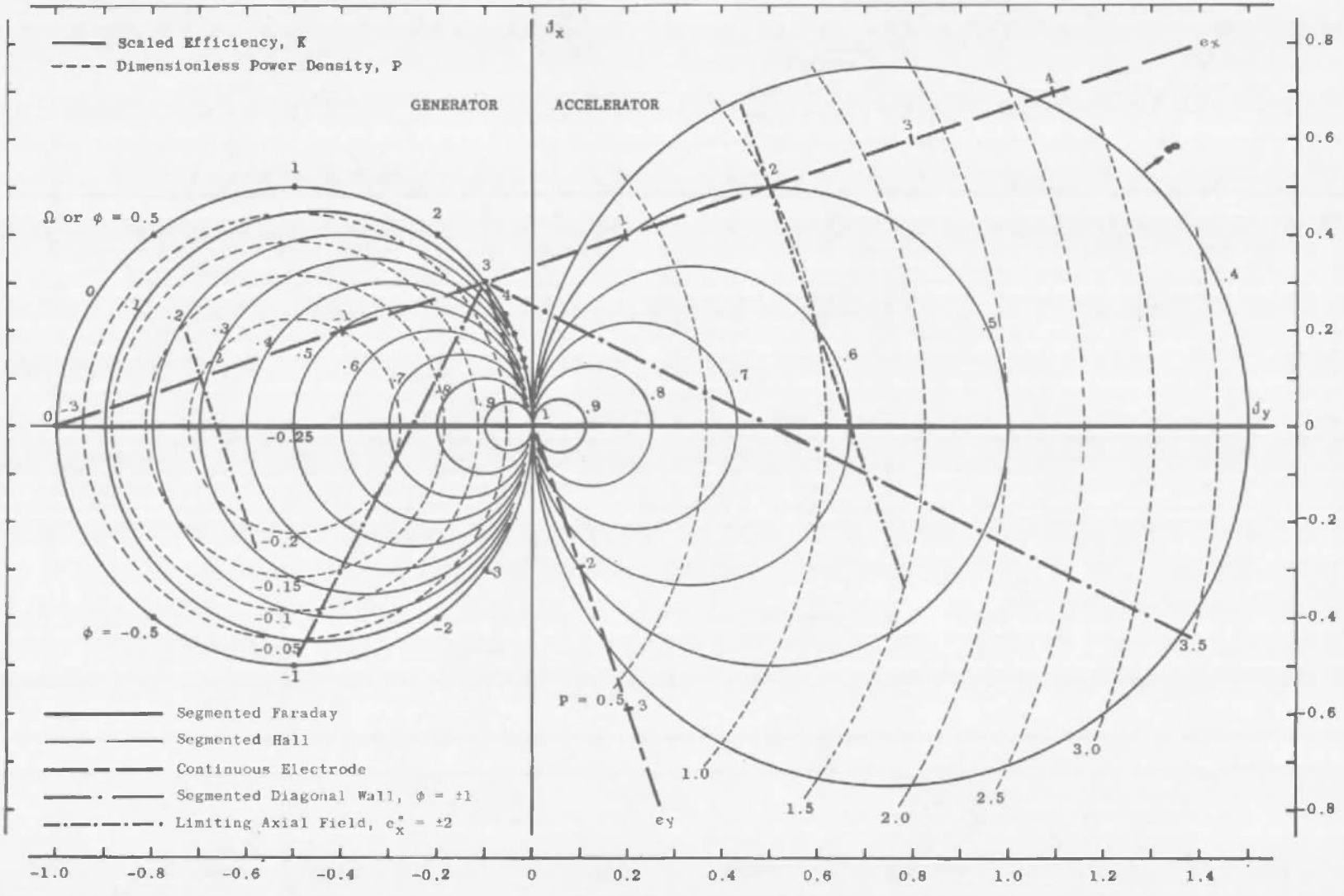

Fig. 7 Comparison of Special Devices

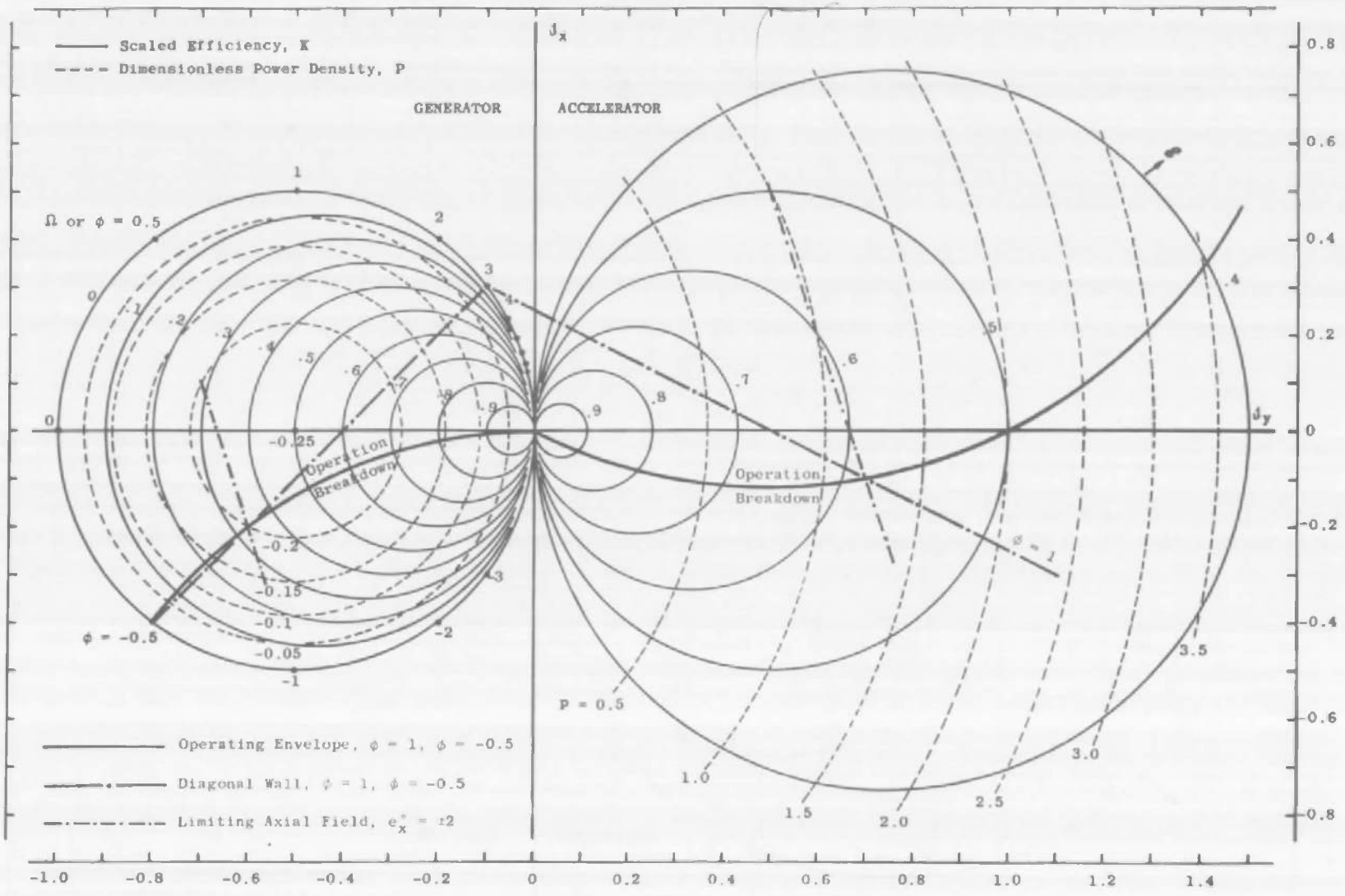

Fig. 8 Axial Field Limited, Diagonal Wall Operating Regimes

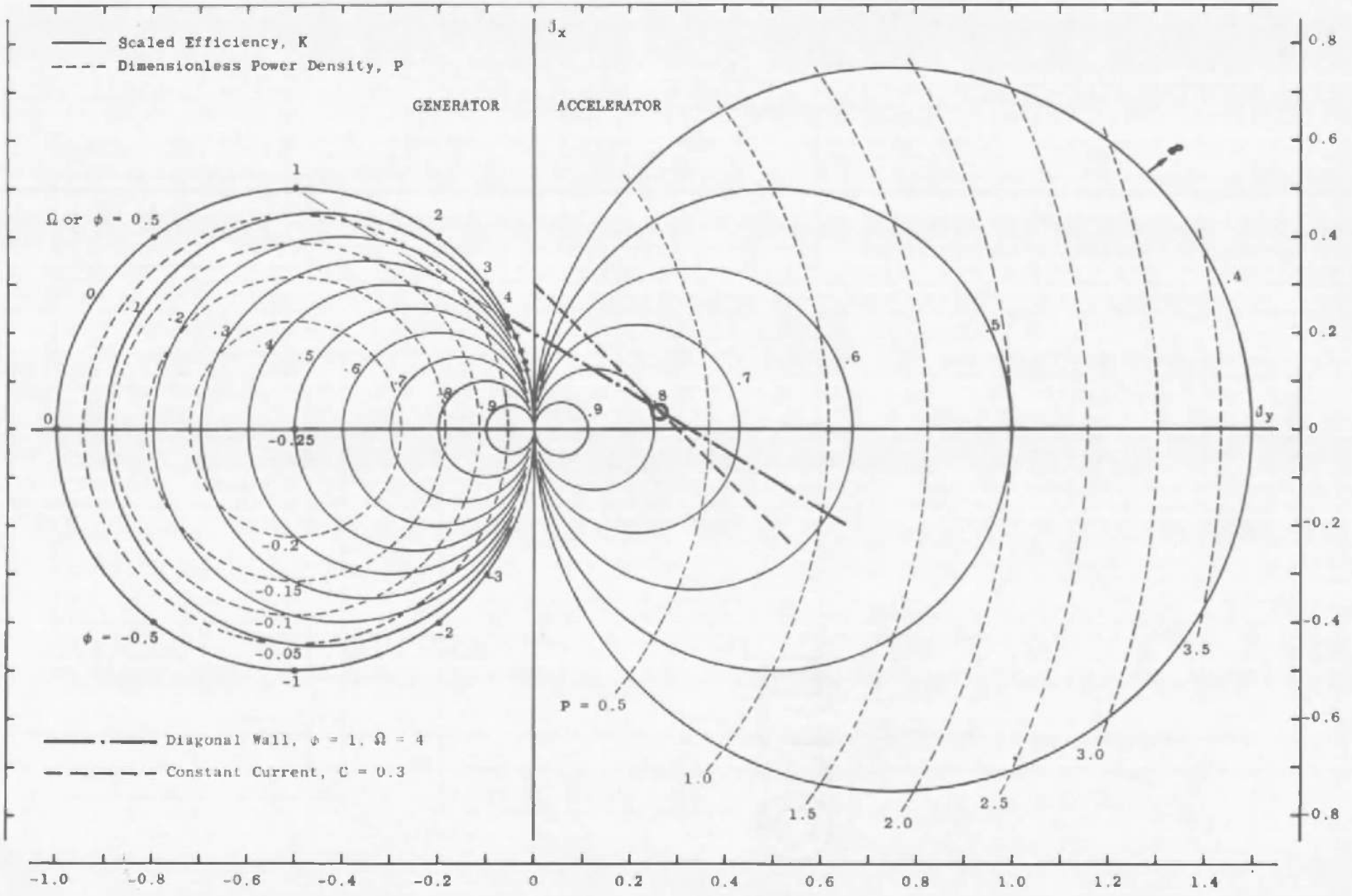

Fig. 9 Constant Total Current, Diagonal Wall Accelerator Operating Point

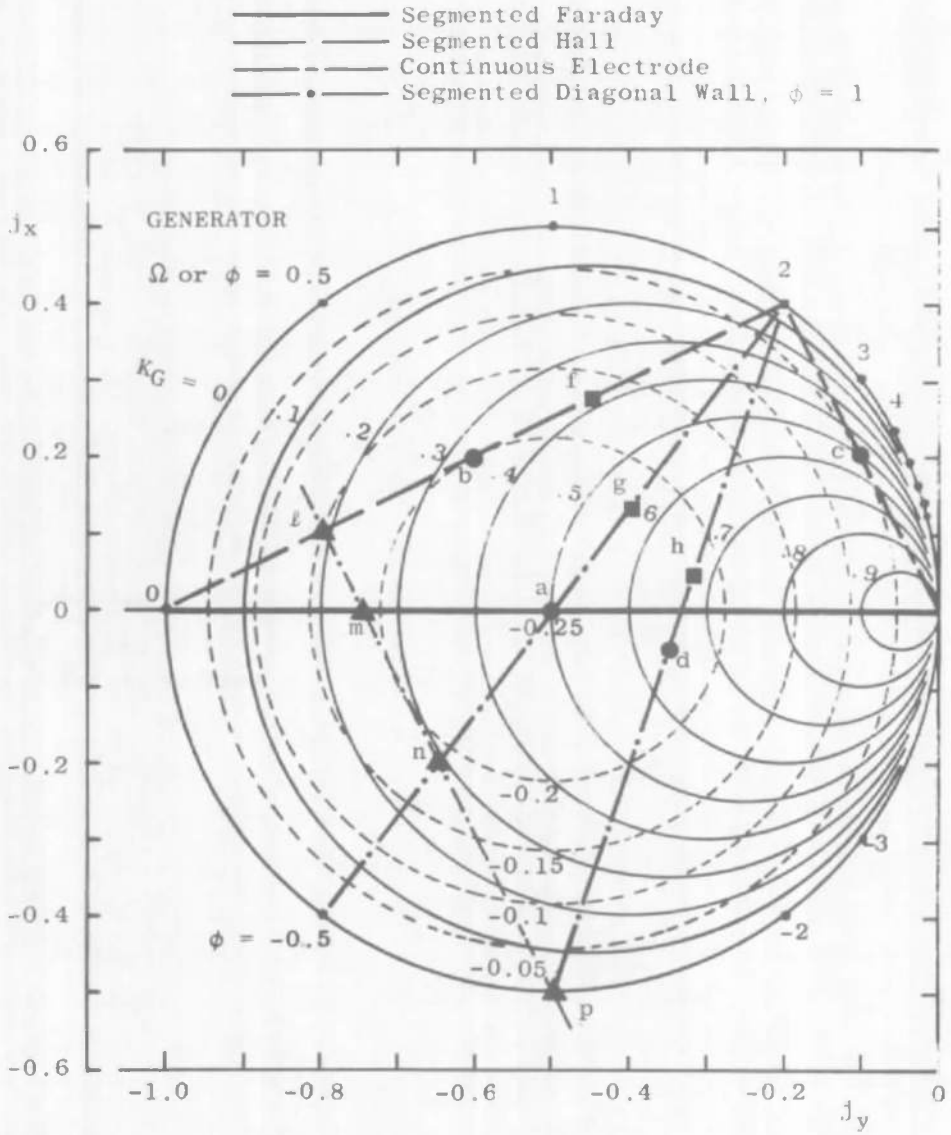

Point	K_G	-P	$-e_x$	e_y	j_x	$-j_y$
a	0.50	0.25	1.0	0.50	0	0.50
b	0.33	0.20	1.0	0	0.20	0.60
c	0.50	0.05	0	0.50	0.20	0.10
d	0.64	0.22	0.75	0.75	-0.05	0.35
f	0.38	0.17	0.62	0	0.28	0.45
g	0.55	0.22	0.67	0.33	0.13	0.40
h	0.67	0.21	0.58	0.58	0.05	0.32
ℓ	0.19	0.15	1.50	0	0.10	0.80
m	0.25	0.19	1.50	0.25	0	0.75
n	0.29	0.19	1.50	0.75	-0.20	0.65
p	0.00	0.00	1.50	1.50	-0.50	0.50

Fig. 10 Interesting Points in Generator Selection for $\Omega = 2$

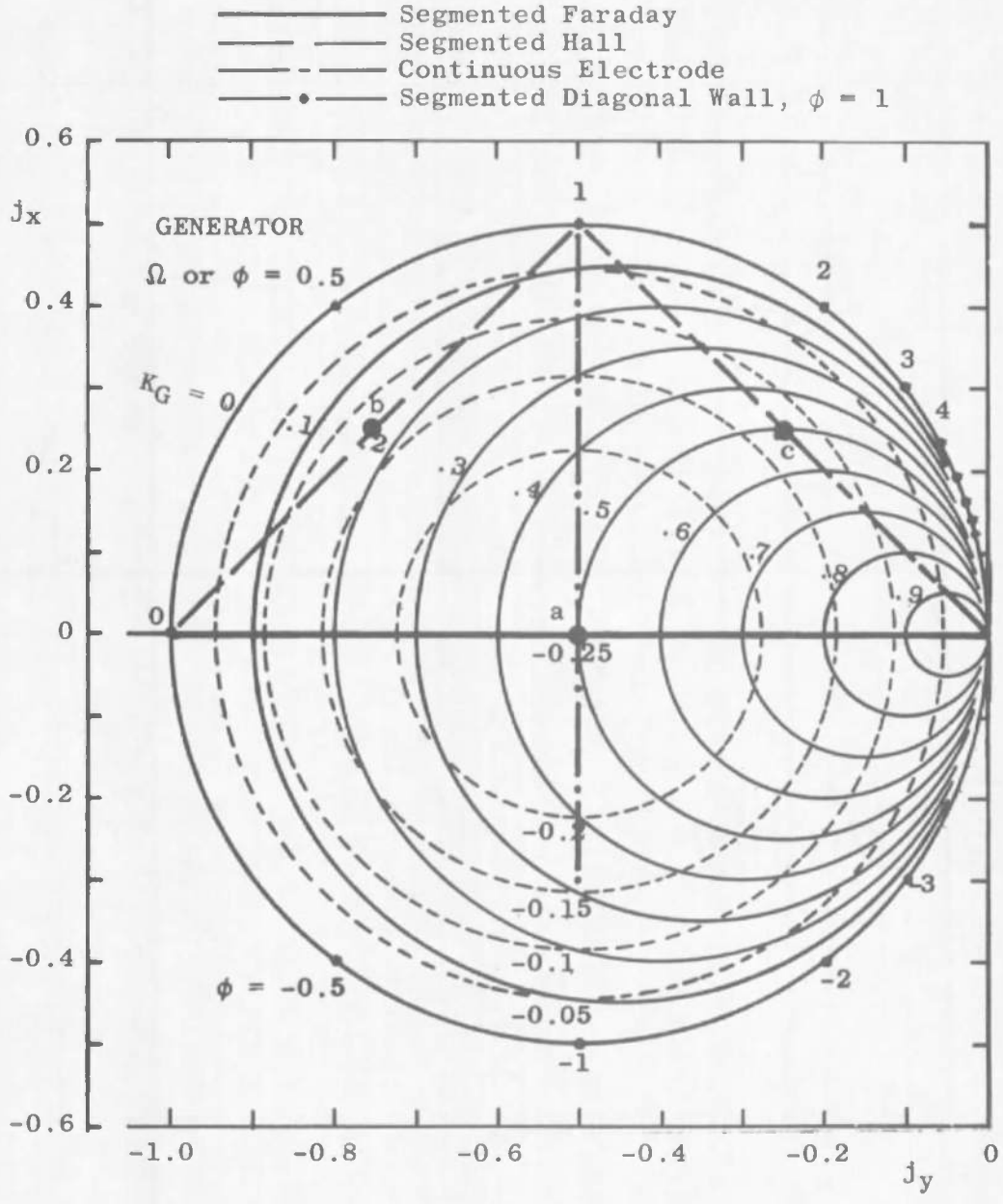

Point	K_G	-P	$-e_x$	e_y	jx	-jy
a	0.50	0.25	0.50	0.50	0	0.50
b	0.17	0.12	0.50	0	0.25	0.75
c	0.50	0.12	0	0.50	0.25	0.25

Fig. 11 Interesting Points in Generotor Selection for $\Omega = 1$

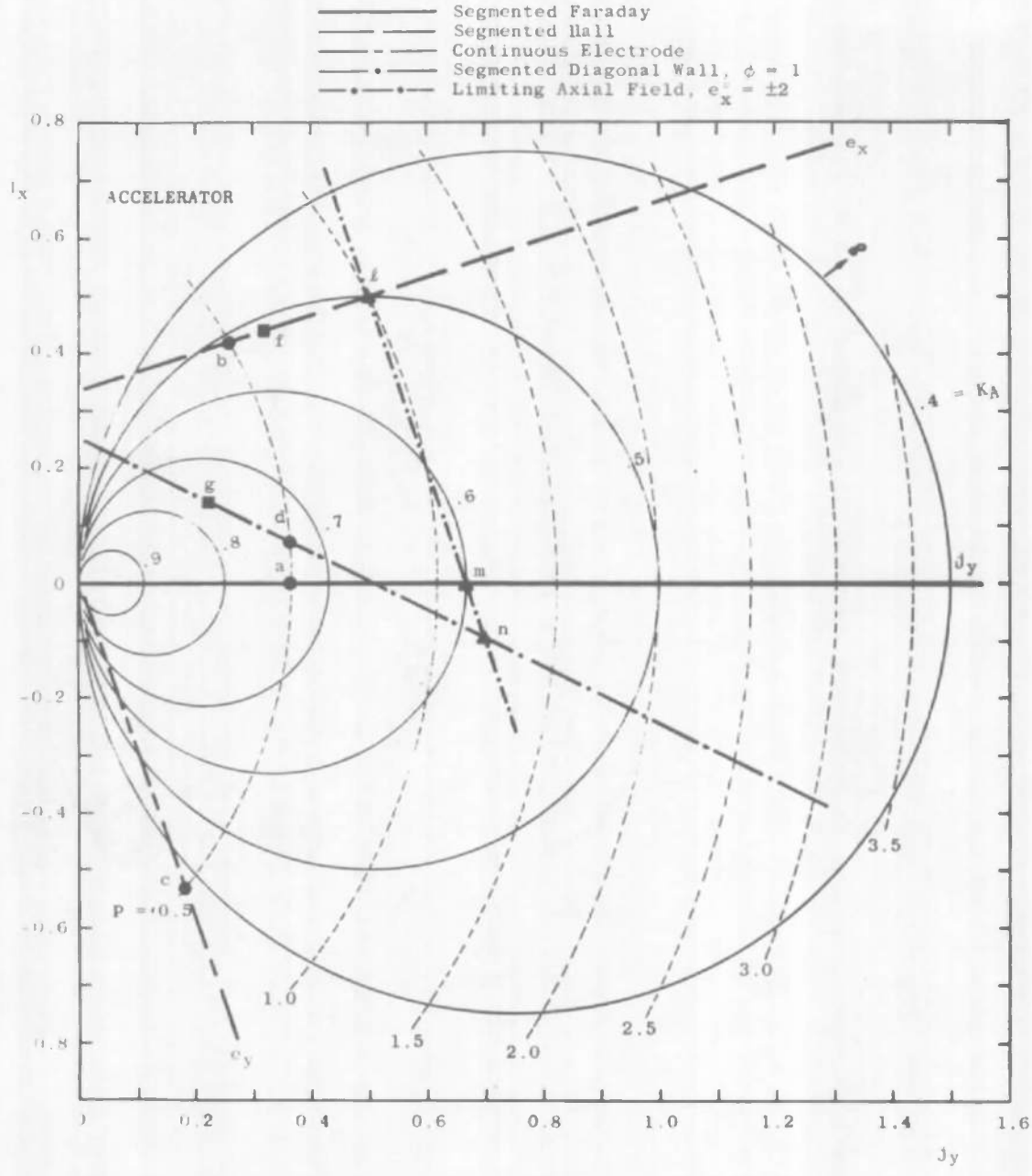

Point	K_A	τ_{iA}	P	e_x	e_y	J_x	J_y
a	0.73	0.49	0.50	1.10	1.37	0	0.37
b	0.52	0.34	0.50	1.19	0	0.42	0.26
c	0.36	0.24	0.50	0	2.79	-0.54	0.13
d	0.73	0.48	0.50	1.16	1.16	0.07	0.36
e	0.52	0.35	0.61	1.39	0	0.44	0.32
g	0.76	0.51	0.29	0.81	0.81	0.14	0.22
k	0.50	0.33	1.00	2.00	0	0.50	0.50
m	0.60	0.40	1.11	2.00	1.67	0	0.67
n	0.53	0.39	1.20	2.00	2.00	-0.10	0.70

Fig. 12 Interesting Points in Accelerator Selection for $\Omega = 3$

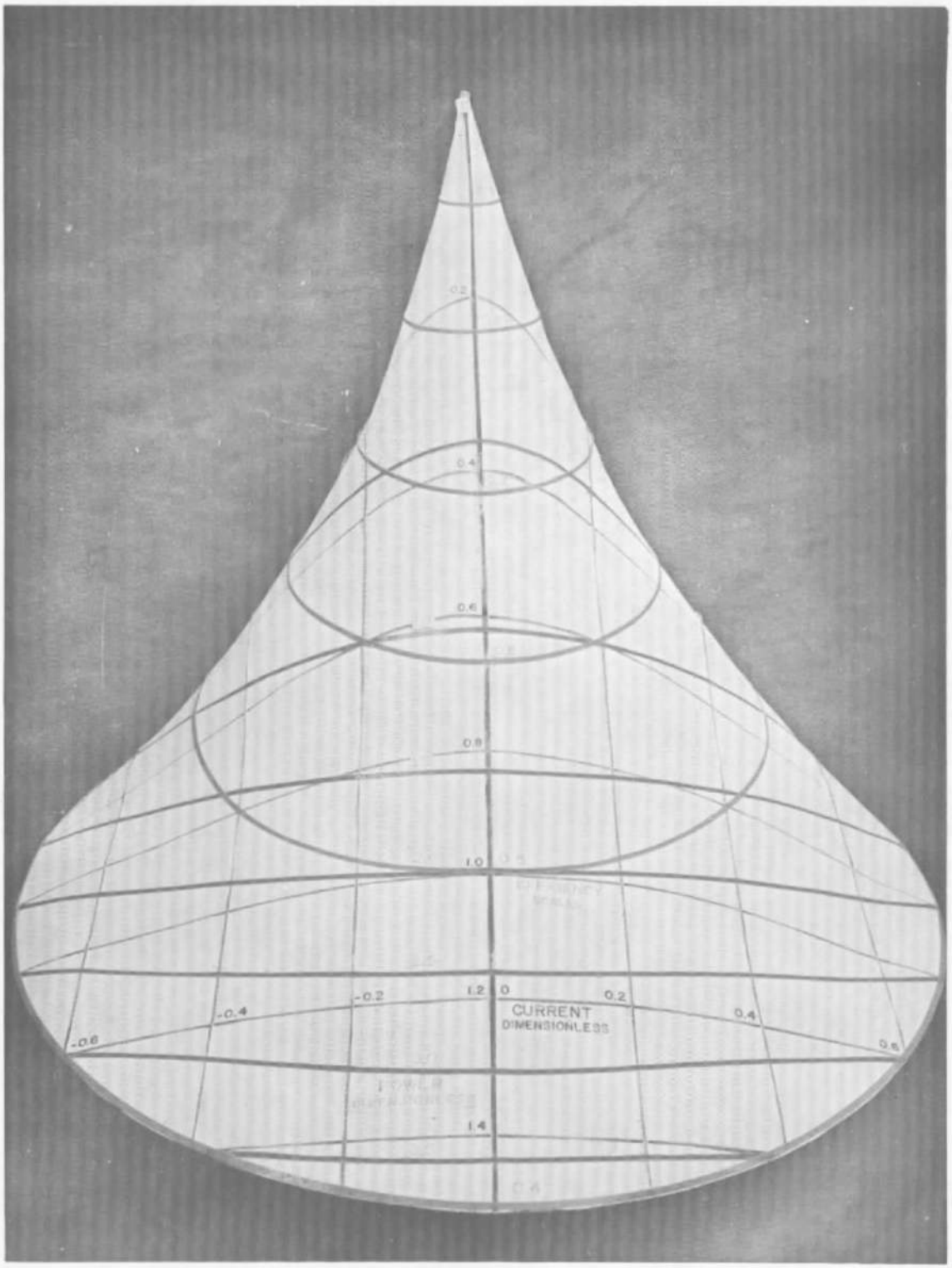

Fig. 13 Photograph of Accelerator Model

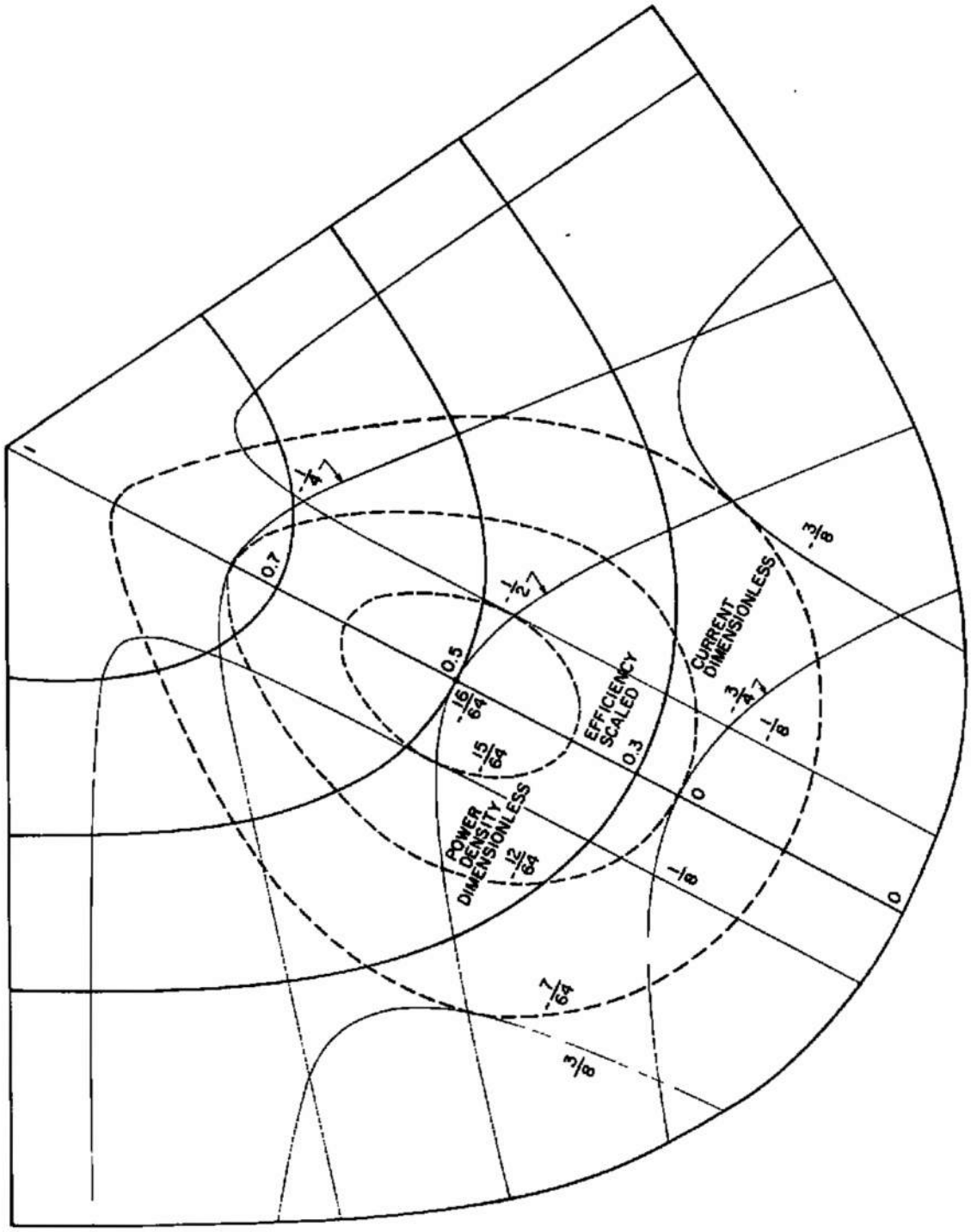

Fig. 14 Development of Generator Model

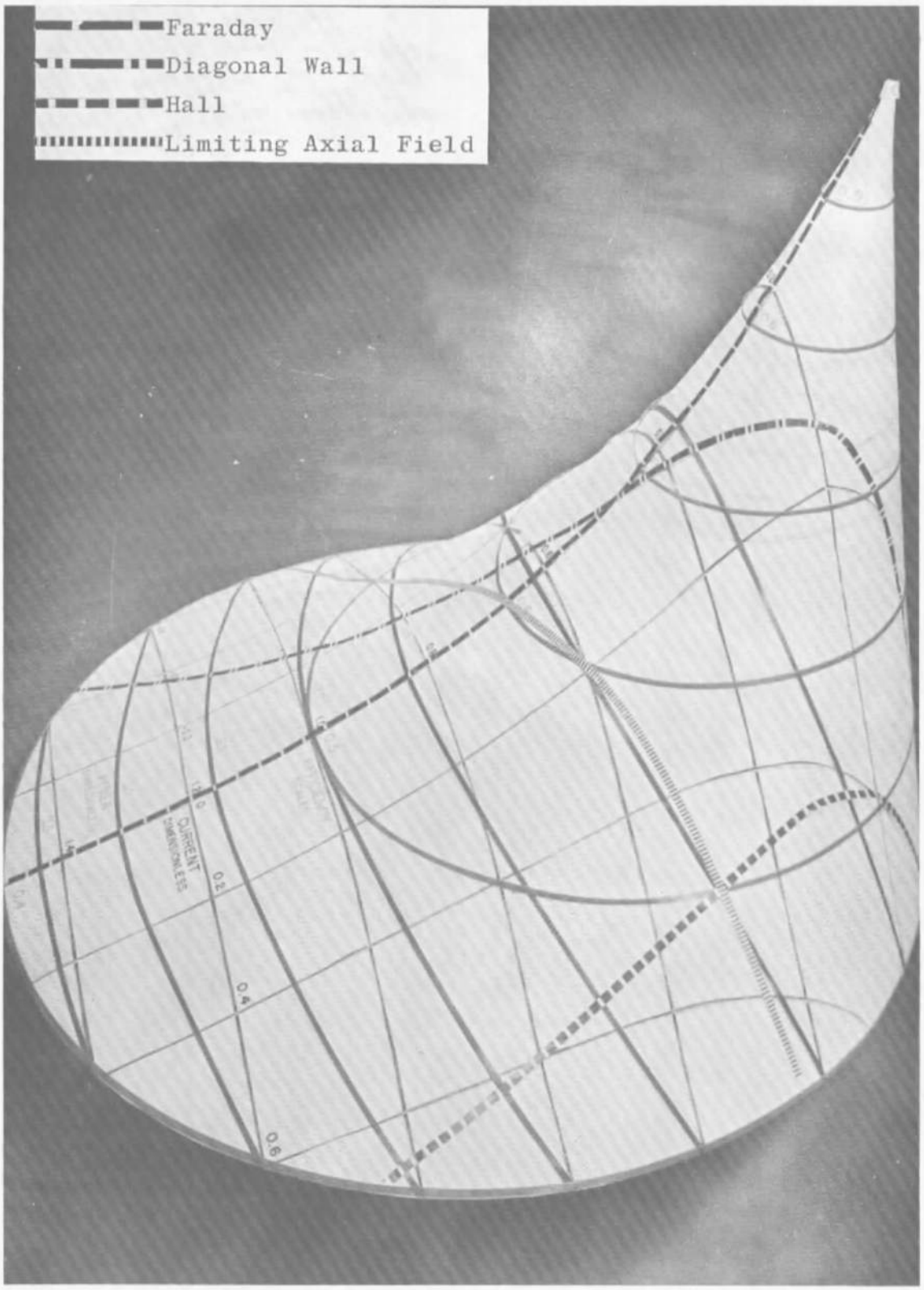

Fig. 15 Photograph of Accelerator Types on Model for $\Omega = 3$

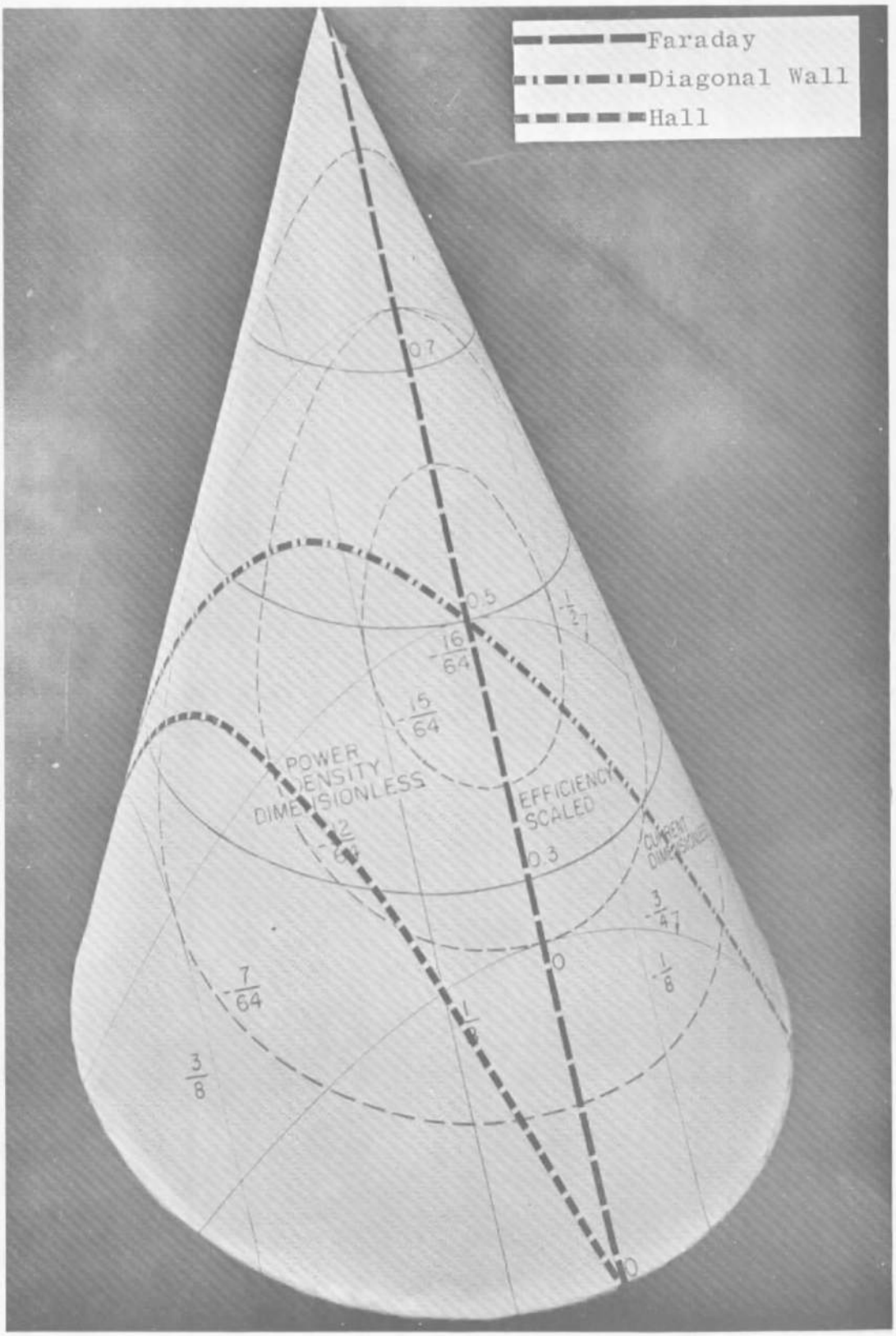

Fig. 16 Photograph of Generator Types on Model for $\Omega = 2$

UNCLASSIFIED

Security Classification

DOCUMENT CONTROL DATA - R&D

(Security classification of title, body of abstract and indexing annotation must be entered when the overall report is classified)

1 ORIGINATING ACTIVITY (Corporate author)
Arnold Engineering Development Center (AEDC)
ARO, Inc. Operating Contractor
Arnold Air Force Station, Tennessee

2a REPORT SECURITY CLASSIFICATION
UNCLASSIFIED

2b GROUP
N/A

3 REPORT TITLE
A GENERALIZED GRAPHICAL PRESENTATION OF MAGNETOHYDRODYNAMIC ACCELERATOR AND GENERATOR PERFORMANCE CHARACTERISTICS

4 DESCRIPTIVE NOTES (Type of report and inclusive dates)
N/A

5. AUTHOR(S) (Last name, first name, initial)
Powers, W. L. ARO, Inc.
Dicks, J. B. and Snyder, W. T., University of Tenn. Space Institute

6. REPORT DATE	7a. TOTAL NO. OF PAGES	7b. NO. OF REFS
October 1965	44	12

8a. CONTRACT OR GRANT NO. AF 40(600)-1200

b. PROJECT NO. 7778

c. Program Element 624110034

d Task 777805

9a. ORIGINATOR'S REPORT NUMBER(S)
AEDC-TR-65-193

9b. OTHER REPORT NO(S) (Any other numbers that may be assigned this report)
N/A

10. AVAILABILITY/LIMITATION NOTICES
Qualified requesters may obtain copies of this report from DDC.

11. SUPPLEMENTARY NOTES
N/A

12. SPONSORING MILITARY ACTIVITY
Arnold Engineering Development Center (AEDC), Air Force Systems Command (AFSC), Arnold AF Station, Tenn.

13. ABSTRACT

This report presents a graphical display of the generalized Ohm's law which is assumed to describe the local electrical characteristics of magnetohydrodynamic accelerators and generators. Sheath voltage drops and ion slip are included, but viscous effects are excluded. A performance map is presented in terms of dimensionless electrical quantities. The features of the continuous electrode, segmented Faraday, segmented diagonal conducting wall, and segmented Hall accelerators and generators are represented on the same performance map for purposes of comparison. The operating equations pertinent to each of the special devices are also derived and expressed in terms of the dimensionless quantities. It is shown how this map may be used in evaluating MHD channel performance and how it materially aids in channel design and in selecting the most desirable kind of device for a given set of specifications.

DD FORM 1 JAN 64 1473

UNCLASSIFIED

Security Classification

14 KEY WORDS	LINK A		LINK B		LINK C	
	ROLE	WT	ROLE	WT	ROLE	WT
magnetohydrodynamics accelerators generators performance						

INSTRUCTIONS

1. ORIGINATING ACTIVITY: Enter the name and address of the contractor, subcontractor, grantee, Department of Defense activity or other organization *(corporate author)* issuing the report.

2a. REPORT SECURITY CLASSIFICATION: Enter the overall security classification of the report. Indicate whether "Restricted Data" is included. Marking is to be in accordance with appropriate security regulations.

2b. GROUP: Automatic downgrading is specified in DoD Directive 5200.10 and Armed Forces Industrial Manual. Enter the group number. Also, when applicable, show that optional markings have been used for Group 3 and Group 4 as authorized.

3. REPORT TITLE: Enter the complete report title in all capital letters. Titles in all cases should be unclassified. If a meaningful title cannot be selected without classification, show title classification in all capitals in parenthesis immediately following the title.

4. DESCRIPTIVE NOTES: If appropriate, enter the type of report, e.g., interim, progress, summary, annual, or final. Give the inclusive dates when a specific reporting period is covered.

5. AUTHOR(S): Enter the name(s) of author(s) as shown on or in the report. Enter last name, first name, middle initial. If military, show rank and branch of service. The name of the principal author is an absolute minimum requirement.

6. REPORT DATE: Enter the date of the report as day, month, year, or month, year. If more than one date appears on the report, use date of publication.

7a. TOTAL NUMBER OF PAGES: The total page count should follow normal pagination procedures, i.e., enter the number of pages containing information.

7b. NUMBER OF REFERENCES: Enter the total number of references cited in the report.

8a. CONTRACT OR GRANT NUMBER: If appropriate, enter the applicable number of the contract or grant under which the report was written.

8b, 8c, & 8d. PROJECT NUMBER: Enter the appropriate military department identification, such as project number, subproject number, system numbers, task number, etc.

9a. ORIGINATOR'S REPORT NUMBER(S): Enter the official report number by which the document will be identified and controlled by the originating activity. This number must be unique to this report.

9b. OTHER REPORT NUMBER(S): If the report has been assigned any other report numbers *(either by the originator or by the sponsor)*, also enter this number(s).

10. AVAILABILITY/LIMITATION NOTICES: Enter any limitations on further dissemination of the report, other than those imposed by security classification, using standard statements such as:

(1) "Qualified requesters may obtain copies of this report from DDC."

(2) "Foreign announcement and dissemination of this report by DDC is not authorized."

(3) "U. S. Government agencies may obtain copies of this report directly from DDC. Other qualified DDC users shall request through _____."

(4) "U. S. military agencies may obtain copies of this report directly from DDC. Other qualified users shall request through _____."

(5) "All distribution of this report is controlled. Qualified DDC users shall request through _____."

If the report has been furnished to the Office of Technical Services, Department of Commerce, for sale to the public, indicate this fact and enter the price, if known.

11. SUPPLEMENTARY NOTES: Use for additional explanatory notes.

12. SPONSORING MILITARY ACTIVITY: Enter the name of the departmental project office or laboratory sponsoring *(paying for)* the research and development. Include address.

13. ABSTRACT: Enter an abstract giving a brief and factual summary of the document indicative of the report, even though it may also appear elsewhere in the body of the technical report. If additional space is required, a continuation sheet shall be attached.

It is highly desirable that the abstract of classified reports be unclassified. Each paragraph of the abstract shall end with an indication of the military security classification of the information in the paragraph, represented as *(TS)*, *(S)*, *(C)*, or *(U)*.

There is no limitation on the length of the abstract. However, the suggested length is from 150 to 225 words.

14. KEY WORDS: Key words are technically meaningful terms or short phrases that characterize a report and may be used as index entries for cataloging the report. Key words must be selected so that no security classification is required. Identifiers, such as equipment model designation, trade name, military project code name, geographic location, may be used as key words but will be followed by an indication of technical context. The assignment of links, rules, and weights is optional.